© 2016. Published by The Company of Biologists Ltd | Development (2016) 143, 2206-2216 doi:10.1242/dev.132357

RESEARCH ARTICLE

Tcf7l1 protects the anterior neural fold from adopting the neural crest fate

Jan Mašek[1], Ondřej Machoň[1,*], Vladimír Kořínek[1], M. Mark Taketo[2] and Zbyněk Kozmik[1]

ABSTRACT

The neural crest (NC) is crucial for the evolutionary diversification of vertebrates. NC cells are induced at the neural plate border by the coordinated action of several signaling pathways, including Wnt/β-catenin. NC cells are normally generated in the posterior neural plate border, whereas the anterior neural fold is devoid of NC cells. Using the mouse model, we show here that active repression of Wnt/β-catenin signaling is required for maintenance of neuroepithelial identity in the anterior neural fold and for inhibition of NC induction. Conditional inactivation of Tcf7l1, a transcriptional repressor of Wnt target genes, leads to aberrant activation of Wnt/β-catenin signaling in the anterior neuroectoderm and its conversion into NC. This reduces the developing prosencephalon without affecting the anterior-posterior neural character. Thus, Tcf7l1 defines the border between the NC and the prospective forebrain via restriction of the Wnt/β-catenin signaling gradient.

KEY WORDS: Tcf/Lef, Wnt signaling, Neural crest, Forebrain, Mouse, Zebrafish

INTRODUCTION

Neural crest (NC) cells are vertebrate-specific, multipotent, highly migratory cells that originate from the ectoderm of the neural plate border (NPB). NC cells possess the ability to differentiate into a wide range of cell types, including the bone and cartilage of the skull, sensory neurons, outflow tract of the heart, enteric ganglia and pigment cells. During embryogenesis, a combination of gene expression driven by Wnt, FGF and BMP pathways determines the future characteristics of the head ectoderm, transforming it into either placodes, neural plate, epidermis or NC cells (Garnett et al., 2012; Groves and LaBonne, 2014; Litsiou et al., 2005; Simoes-Costa and Bronner, 2015; Steventon et al., 2009). Wnt/β-catenin represents one of the most extensively studied signaling cascades. Binding of secreted Wnt proteins to their Frizzled receptors and their Lrp5/6 co-receptors initiates a complex cascade of intracellular events leading to the stabilization of β-catenin. Stabilized β-catenin accumulates in the cytoplasm and enters the nucleus, where it binds to the Tcf/Lef family of transcription factors, thereby regulating the expression of Wnt target genes (Clevers and Nusse, 2012; http://web.stanford.edu/group/nusselab/cgi-bin/wnt/).

Four Tcf/Lef genes have been identified in vertebrates: *Lef1* (Travis et al., 1991), *Tcf7* (alias *Tcf1*) (van de Wetering et al., 1991), *Tcf7l1* and *Tcf7l2* (alias *Tcf3* and *Tcf4*) (Castrop et al., 1992). Tcf/Lefs share several characteristic protein features, such as the N-terminal β-catenin-binding motif, GRG motifs for binding of Groucho/TLE co-repressors, and the HMG box containing the DNA-binding domain. Tcf7 and Tcf7l2 also contain a C-clamp, a second DNA-binding motif that further modulates gene target specificity (Cadigan and Waterman, 2012). Distinct expression patterns of individual Tcf/Lefs and their unequal capability to activate/repress Wnt target genes represent the ultimate regulatory step of the Wnt/β-catenin signaling pathway. Tcf7l1, expressed in the anterior ectoderm at E7.5 and in the anterior neural fold (ANF) at E8.5 of the developing mouse embryo (Korinek et al., 1998; Merrill et al., 2004), is the least potent activator but the strongest repressor of the whole family (Cole et al., 2008; Liu et al., 2005; Ombrato et al., 2012). Tcf7l1-deficient mice, which display a duplicated axis and a severely reduced anterior part of the embryo, die shortly after gastrulation (Merrill et al., 2004). Tcf7l1 inactivation appears to allow Wnt/β-catenin signaling to spread towards the ANF in both zebrafish and mouse. This leads to a deficiency in the expression of ANF-specific genes, accompanied by severe defects in head formation (Andoniadou et al., 2011; Dorsky et al., 2003; Kim et al., 2000). All these data have been interpreted as consistent with the repression of Wnt signaling in the ANF being required for anterior-posterior (A-P) axis determination of the neural tube.

Experiments in *Xenopus*, zebrafish and chicken have shown a requirement for Wnt/β-catenin signaling from the earliest steps of NC development, at first during gastrulation when Wnt/β-catenin signaling drives the expression of the NC specifier genes *Pax3* (Bang et al., 1999; Garnett et al., 2012; Taneyhill and Bronner-Fraser, 2005; Zhao et al., 2014), *Foxd3* (Janssens et al., 2013) and *Gbx2* (Li et al., 2009), and later during NC maintenance (Kléber et al., 2005; Steventon et al., 2009) and the epithelial-to-mesenchymal transition (EMT), via triggering *Slug* (*Snai2*, or *Snail2*) gene expression (Burstyn-Cohen et al., 2004; Sakai et al., 2005; Vallin et al., 2001). In contrast to non-mammalian experimental models, a clear picture of the role of Wnt/β-catenin signaling in early NC cell populations in mammals is absent. This is partly caused by a lack of appropriate Cre drivers for the early pre-migratory NC lineage. The widely used *Wnt1-Cre* mouse targets the NC population after its induction and specification (Danielian et al., 1998; Lewis et al., 2013). Depletion of β-catenin using *Wnt1-Cre* leads to malformations of the craniofacial structures, accompanied with a deficiency in sensory neurons (Brault et al., 2001; Gay et al., 2015). Similar phenotypic changes have been observed in compound *Wnt1*/*Wnt3a* mutants, which also show impaired formation of sensory neurons and defects in several bones and cartilage derived from the NC (Ikeya et al., 1997). Ectopic *Wnt1-Cre*-driven expression of stabilized β-catenin (*β-cat*$^{Ex3fl/+}$) results in excessive differentiation of NC progenitors into NeuroD (Neurod1) and Brn3a (Pou4f1) positive sensory neurons, thus limiting NC

[1]Institute of Molecular Genetics, Academy of Science of the Czech Republic, Prague 142 20, Czech Republic. [2]Department of Pharmacology, Graduate School of Medicine, Kyoto University, Kyoto 606-8501, Japan.

*Author for correspondence (machon@img.cas.cz)

O.M., 0000-0002-5139-1406

Received 23 October 2015; Accepted 21 April 2016

Development (2016) 143, 2206-2216 doi:10.1242/dev.132357

multipotency (Lee et al., 2004). Collectively, these data confirm the requirement of Wnt/β-catenin signaling in NC maintenance and differentiation; however, they do not clarify the role of Wnts in NC induction and specification. The apparent inconsistency might be explained in two ways: (1) the signaling pathway network governing NC induction and specification differs between mouse and other species (Barriga et al., 2015); or (2) the *Wnt1-Cre* driver targets the already specified NC, which does not allow investigation of earlier events of NC development.

The aim of this work was to investigate the role of Wnt/β-catenin signaling in the early development of the mammalian NC. We used a Cre line derived from the NC inducer gene *Tfap2a* (*AP2α-Cre*) (Macatee et al., 2003), in order to achieve conditional deletion of *Tcf7l1* in the earliest stages of NC development. Conditional inactivation of *Tcf7l1* leads to transdifferentiation of ANF into NC cells, accompanied by loss of anterior neural markers. Our data suggest that Tcf7l1, acting as a Wnt/β-catenin repressor, is required to maintain anterior neural character by restricting expansion of the Wnt-induced NC cells.

RESULTS

AP2α-Cre-mediated deletion of *Tcf7l1* during mouse NC specification results in exencephaly

Tcf7l1 is detected in the developing mouse ectoderm prior to gastrulation and later, at E7.5, it is expressed in the anterior ectoderm and mesoderm (Korinek et al., 1998; Merrill et al., 2004). We characterized the expression of *Tcf7l1* during neurulation using whole-mount *in situ* hybridization. *Tcf7l1* mRNA was detected in the anterior neural plate at the one somite pair (s) stage, being further restricted to the ANF region and along the anterior NPB with the progress of neurulation at 3-4 s stage (Fig. 1A). We next aimed to relate the expression pattern of *Tcf7l1* to that of known NC-specific genes and the area of Wnt/β-catenin signaling. *Tfap2a* is one of the key genes involved in NC induction, while *Foxd3*, *Sox9* and *Sox10* have been linked with NC specification (Groves and LaBonne, 2014; Simoes-Costa and Bronner, 2015). During neurulation Tfap2α protein is continuously expressed along the whole NPB, as shown by whole-mount immunofluorescence (Fig. 1B). First, *Sox9* and *Foxd3* transcripts were detected in the neural plate as early

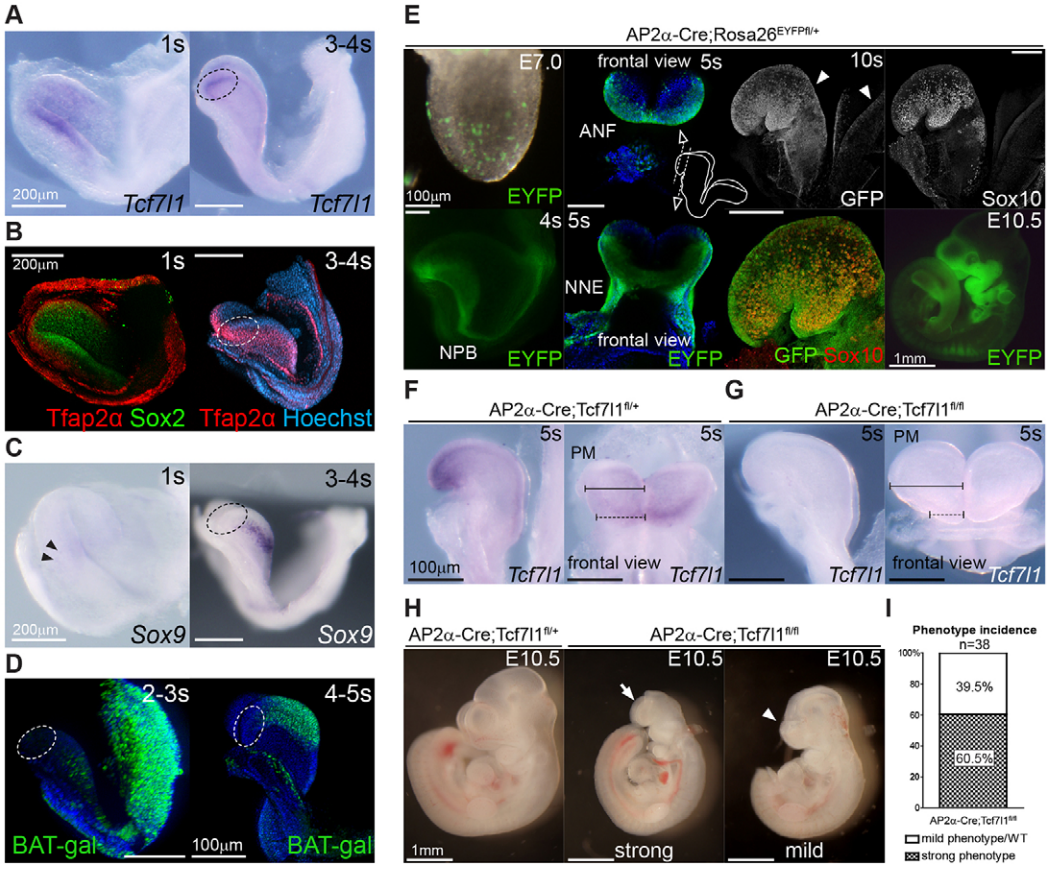

Fig. 1. Tcf7l1 is expressed in a mutually exclusive manner with markers of specified NC and is required for proper forebrain development. (A-D) Expression of *Tcf7l1* mRNA, the neuroectoderm marker Sox2, early NC marker Tfap2α, *Sox9* mRNA as a marker of specified NC, and the Wnt reporter BAT-gal in the NPB and the ANF (encircled) of the mouse embryo between 1 and 5 somite pairs (s). Note the overlap of *Tcf7l1* transcripts with Tfap2α protein, and of *Sox9* mRNA with BAT-gal signal. Arrowheads (C) indicate *Sox9* transcripts in the neural plate. (E) Mapping of recombination delivered by AP2α-Cre using *Rosa26*$^{EYFPfl/+}$ reporter mice at various stages (E7.0-E10.5). EYFP was detected either directly or using anti-GFP antibody. Two different optical sections from the frontal view of the 5 s embryo are displayed (open arrowheads). The recombination occurred along the entire NPB (arrowheads, 10 s stage). Overlapping staining of GFP and Sox10 confirms recombination in the whole cranial NC population at the 10 s stage. (F,G) *In situ* hybridization shows the loss of *Tcf7l1* mRNA expression in *AP2α-Cre;Tcf7l1*$^{fl/fl}$ mutants at 5 s stage. Neurectoderm is broader in the region of the prosencephalic-mesencephalic boundary (solid bar), whereas the anterior tip of the ANF is narrower (dashed bar) in the mutants. (H) Control embryo (left) and typical examples of 'strong' (middle) and 'mild' (right) *AP2α-Cre;Tcf7l1*$^{fl/fl}$ phenotype. Arrow, severe reduction of the telencephalic tissue and exencephaly in the strong phenotype; arrowhead, reduced telencephalon and bilateral anopthalmia in the mild phenotype. (I) Quantification of strong and mild phenotype incidence between E10.5 and E13.5. ANF, anterior neural fold; NPB, neural plate border; NNE, non-neural ectoderm; PM, prosencephalic-mesencephalic boundary. Embryos are shown from a lateral view unless stated otherwise. Nuclei were stained with Hoechst. See also Fig. S1.

Development (2016) 143, 2206-2216 doi:10.1242/dev.132357

as the 1-2 s stage (Fig. 1C, Fig. S1A), and at 3-4 s they were expressed robustly in two stripes along the anterior NPB (Fig. 1C, Fig. S1A). The onset of *Sox10* mRNA was detected later (4-5 s), in a pattern overlapping with *Sox9* and *Foxd3* expression (Fig. S1B). To map the activity of the Wnt/β-catenin pathway, we used BAT-gal reporter mice (Maretto et al., 2003). The BAT-gal signal, visualized by immunostaining, was found to spread gradually across the prospective mesencephalon and metencephalon from 2-3 s to 4-5 s stage, but it was never detected in the ANF (Fig. 1D). In conclusion, *Tcf7l1* expression in the ANF overlaps with that of Tfap2α in the anterior part of the NPB but it is reciprocal to that of *Sox9*, *Foxd3*, *Sox10* and BAT-gal, which reside in the caudal areas of the neural plate.

In order to study the function of Tcf7l1 during NC induction and specification, we inactivated Tcf7l1 by crossing *Tcf7l1* conditional knockout mice (EUCOMM) with *AP2α-IRESCre* (*AP2α-Cre*) transgenics (Macatee et al., 2003). Tracing of the *AP2α-Cre*-driven recombination using the *Rosa26*$^{EYFPfl/+}$ reporter strain revealed the first EYFP^{+} cells scattered throughout the embryo at E7.0 (Fig. 1E). The EYFP signal became focused along the entire NPB at the 4 s stage, with the highest levels detected rostrally in the neural- and non-neural ectoderm of the ANF at the 5 s stage. AP2α-Cre most likely targets the entire NC population because all Sox10^{+} NC cells were included in the EYFP^{+} tissue of *AP2α-Cre;Rosa26*$^{EYFPfl/+}$ embryos at the 10 s stage (Fig. 1E). At E10.5, the EYFP signal was present in NC derivatives (brachial arches, dorsal root ganglia and sensory neurons), the head ectoderm, lens placodes, and in the anterior telencephalon (Fig. 1E, Fig. S1C).

In *AP2α-Cre;Tcf7l1*$^{fl/fl}$ mutants, *Tcf7l1* mRNA was completely lost, whereas control embryos showed high levels of transcripts along the anterior NPB including the ANF at the 5 s stage (Fig. 1F,G). At this stage, phenotypic changes following *Tcf7l1* deletion became apparent: neural folds narrowed and the neural plate expanded laterally at the prosencephalic-mesencephalic boundary (Fig. 1F,G). Later, at E10.5, we observed a variability in the penetrance of morphological changes among individual mutants. We classified these defects into two categories (Fig. 1H): (1) a 'strong' phenotype, represented by a severe reduction of the telencephalic tissue and exencephaly; and (2) a 'mild' phenotype, with reduced telencephalon and bilateral anopthalmia. Quantification of phenotype incidence between E10.5 and E13.5 revealed that the strong phenotype was present in 60.5% and the mild phenotype in 39.5% of the embryos analyzed (n=38) (Fig. 1I). Mutant embryos with the strong phenotype did not survive beyond E13.5, exhibiting massive exencephaly and severe defects in craniofacial structures (Fig. S1D,E). These data demonstrate that Tcf7l1 function in the ANF is crucial for the development of the mouse forebrain.

Tcf7l1 is required for the expression of anterior neural markers

Tcf7l1 has been implicated in A-P patterning of the developing brain in both zebrafish and mouse, since loss-of-function mutations result in severe reductions of anterior neural regions, accompanied by apparent expansion of midbrain and hindbrain markers towards the anterior (Dorsky et al., 2003; Merrill et al., 2004). In contrast to published data, we did not observe any A-P shift in mRNA expression of the core regulators of the midbrain-hindbrain boundary (MHB) *Fgf8*, *Gbx2* and *Wnt1* between *Tcf7l1* conditional mutants and controls at E9.0 (Fig. 2A-B′, Fig. S3B). However, we did observe a progressive loss of the posterior prosencephalon marker *Tcf7l2* mRNA (Fig. 2C-C″), illustrating a

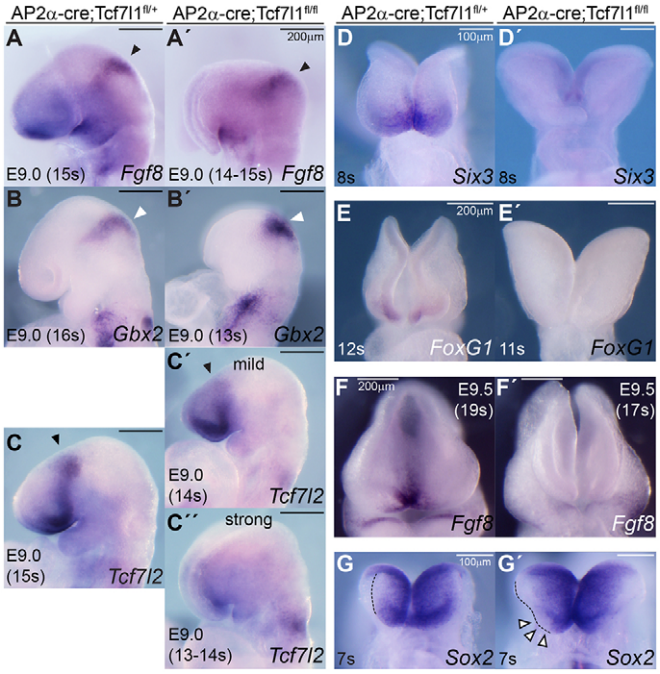

Fig. 2. *Tcf7l1* deletion induces loss of ANF specifiers without affecting posterior brain structures. (A-B′) *In situ* hybridization shows unchanged expression of *Fgf8* and *Gbx2* mRNA in the midbrain-hindbrain boundary (MHB) (arrowheads). Lateral views. (C-C″) *Tcf7l2* mRNA (arrowheads) in the posterior prosencephalon of control and *AP2α-Cre;Tcf7l1*$^{fl/fl}$ mouse embryos displaying mild or strong phenotype at E9.0. Lateral views. (D-G′) *Tcf7l1* deletion results in marked reduction of *Six3* and *Sox2* mRNA expression at 7-8 s stage, *Foxg1* at 11-12 s stage and of *Fgf8* at E9.5 in the ANF of *AP2α-Cre;Tcf7l1*$^{fl/fl}$ embryos. Frontal views. Arrowheads (G′) indicate the expansion of *Sox2*$^{-}$ cells along the anterior lateral border of the ANF in the *AP2α-Cre;Tcf7l1*$^{fl/fl}$ mutants.

gradual loss of anterior neural tissue in *AP2α-Cre;Tcf7l1*$^{fl/fl}$ mutants with mild (Fig. 2C′) or strong (Fig. 2C″) phenotype at E9.0. Furthermore, expression of the ANF-specific transcripts *Six3* (Lagutin et al., 2003), *Foxg1* (Hanashima et al., 2004) and *Fgf8* (Meyers et al., 1998) was lost or strongly reduced in the mutants at the 8 s, 11 s and 17 s stage (E9.5), respectively (Fig. 2D-F′). Next, we tested whether the ANF cells in *Tcf7l1* conditional mutants retained their neural character. RNA *in situ* hybridization revealed reduced expression of the general neural marker *Sox2*, and expansion of *Sox2*$^{-}$ cells along the anterior lateral border of the ANF in *AP2α-Cre;Tcf7l1*$^{fl/fl}$ mutants (Fig. 2G,G′), suggesting that these cells have lost their neural identity.

Tcf7l1 deletion results in aberrant transdifferentiation of ANF cells into NC

NC cells need to lose their neuroepithelial character in order to delaminate and migrate towards their target destinations. NC specification, which precedes delamination in *Xenopus* and chicken, is regulated by the transcription factors FoxD3, Sox9 and Sox10 (Cheung et al., 2005; Dottori et al., 2001; Liu et al., 2013). Therefore, we investigated the expression of these three factors in the absence of Tcf7l1.

As can be seen from whole-mount immunostaining, Sox9^{+} NC cells expanded into the Sox1^{+} ANF region in *AP2α-Cre;Tcf7l1*$^{fl/fl}$ mutants compared with controls at the 5 s stage (Fig. 3A). Examination under higher magnification showed decreased neural Sox1 staining towards the anterior part of the mutant embryo. A frontal view of the same embryos clearly showed ectopic Sox9^{+} NC

Development (2016) 143, 2206-2216 doi:10.1242/dev.132357

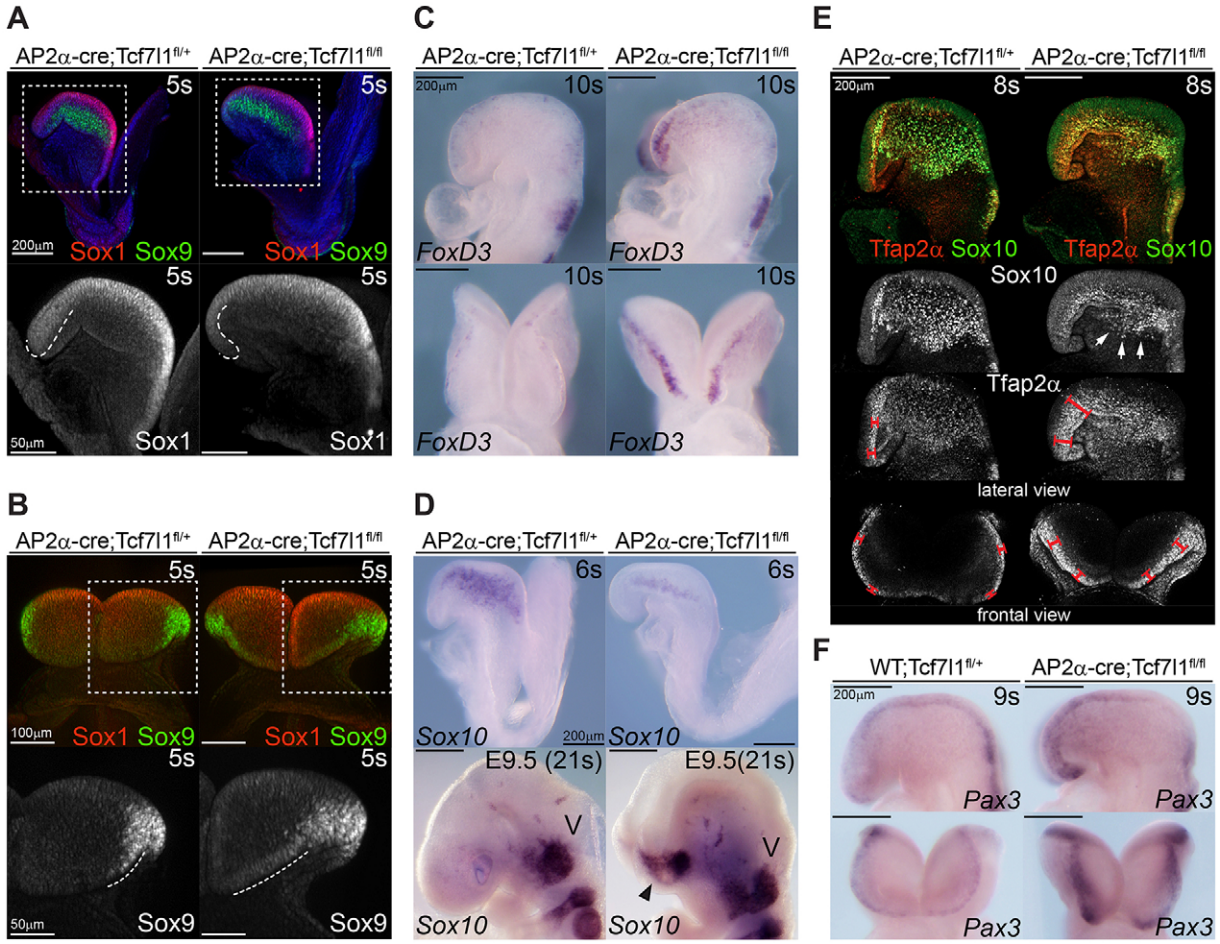

Fig. 3. The NC population expands anteriorly in the absence of Tcf7l1. (A) Whole-mount immunohistochemical staining of Sox1 and Sox9 at 5 s stage. Lateral views. Higher magnification (bottom panels, black and white) revealed reduction of Sox1 staining in the ANF (dashed line) of *AP2α-Cre;Tcf7l1*$^{fl/fl}$ mutants. Nuclei were stained with Hoechst. (B) Frontal views of Sox1 and Sox9 immunofluorescence as in A. Higher magnification documents the expansion (lower panels, dashed line) of Sox9^{+} cells along the ANF border in *AP2α-Cre;Tcf7l1*$^{fl/fl}$ mutants. (C) Ectopic expression of the NC marker *Foxd3* along the ANF of *AP2α-Cre;Tcf7l1*$^{fl/fl}$ mouse embryos at 10 s stage. Lateral (top) and frontal (bottom) views. (D) *Sox10* mRNA is less abundant in *Tcf7l1* conditional mutants at the 6 s stage but becomes ectopically expressed later at E9.5 (bottom panels, arrowhead) in the anterior head of *AP2α-Cre;Tcf7l1*$^{fl/fl}$ mutants. Lateral views. (E) Immunostaining of Sox10 and Tfap2α illustrating the reduced number of Sox10^{+} cells (arrows). The Sox10^{+} population was found to be arrested in the abnormally wide zone of the ANF, which expresses ectopic Tfap2α (bars) in the *AP2α-Cre;Tcf7l1*$^{fl/fl}$ embryos at 8 s stage. Lateral views (top three) and frontal view (bottom). (F) Expression of the NC inducer *Pax3* is strongly increased along the ANF of the mutants when compared with the control embryos at 9 s stage. Lateral (top) and frontal (bottom) views. V, trigeminal ganglion. See also Fig. S2.

cells along the ANF in mutants (Fig. 3B). The loss of the neuroectodermal marker Sox1 was not caused by any increase in apoptosis, as we did not detect any changes in cleaved caspase 3 immunostaining in the mutants at 5 s stage (n=4, Fig. S2A). Upregulation of Sox9 expression was further confirmed by *in situ* hybridization of *Sox9* mRNA (Fig. S2B). Interestingly, we also observed a cell fate shift characterized by the change from Sox1 to Sox9 in the caudal neural tissue. Coronal sectioning of the developing hindbrain at E9.0 also uncovered aberrant Sox9^{+}/Sox1^{-} cells in the mutants (Fig. S2C). Consistent with the ectopic expansion of Sox9-expressing cells, the expression of *Foxd3* was also upregulated along the anterior NPB in *Tcf7l1* conditional mutants at the 10 s stage (Fig. 3C). Later, at E9.0, aberrant *Foxd3* mRNA was detected in the rostral part of the head in mutants (Fig. S2D).

Sox10 mRNA expression was delayed in the absence of Tcf7l1, as it was barely detectable at the 6 s stage, but it emerged in elevated levels one day later at E9.5 in ectopic patches in the anterior part of the malformed head of mutant embryos (Fig. 3D). The onset of *Sox10* expression in *Xenopus* and chicken follows after *Sox9* and *Foxd3*, which appear immediately after NC induction, suggesting its requirement in later events of NC specification (Cheung and Briscoe, 2003; Cheung et al., 2005; McKeown et al., 2005; Sakai et al., 2006). The delay in the onset of *Sox10* expression in the *AP2α-Cre;Tcf7l1*$^{fl/fl}$ mutants could be caused by a prolonged NC induction. To verify this, we analyzed the expression of the key NC inducer Tfap2α (de Croze et al., 2011). Indeed, the region of Tfap2α immunofluorescence was robustly enlarged along the neuroectoderm of the anterior NPB in the *AP2α-Cre;Tcf7l1*$^{fl/fl}$ mutants at the 8 s stage (Fig. 3E). Double staining of Tfap2α together with Sox10 further revealed that only a few Sox10^{+} cells managed to migrate from the NPB in the mutants (Fig. 3E), while the rest of the Sox10 signal appeared to be amassed in the Tfap2α^{+} neuroectoderm of the *Tcf7l1* conditional mutants.

Finally, *Pax3* mRNA signal spread aberrantly along the ANF in a similar way to Tfap2α, Sox9 and *Foxd3* (Fig. 3F). We wanted to confirm this phenomenon in other vertebrates. We co-injected translation-blocking morpholinos (MOs) against zebrafish *tcf7l1a*

Development (2016) 143, 2206-2216 doi:10.1242/dev.132357

and *tcf7l1b* into fertilized zebrafish eggs and stained for *foxd3*, *pax3* and *sox9* mRNA by whole-mount *in situ* hybridization 12 h post-fertilization (hpf). We observed ectopic expression of *foxd3*, *pax3* and *sox9* mRNA along the entire anterior NPB of the *tcf7l1a/b* morphant zebrafish (Fig. S2E). The ectopic NC induction was almost completely rescued by co-injection of mouse *Tcf7l1* mRNA (Fig. S2F).

Taken together, the expression of genes responsible for NC induction and specification was expanded along the ANF in *AP2α-Cre;Tcf7l1*$^{fl/fl}$ mouse mutants and in *tcf7l1* zebrafish morphants. This suggests that Tcf7l1, by forming a boundary to the expression of NC specifiers, maintains the neuroepithelial character of the lateral ANF and restricts NC induction from the anterior head.

Transdifferentiation of the ANF is driven by aberrant Wnt/β-catenin signaling

Tcf7l1 is a very efficient repressor of Wnt/β-catenin signaling target genes, as has been shown in both mouse embryonic stem cells and *in vivo* (Cole et al., 2008; Shy et al., 2013; Wu et al., 2012). Gain- and loss-of-function experiments in non-mammalian vertebrates have shown that the Wnt/β-catenin pathway is required for physiological (and sufficient for ectopic) induction and expansion of the NC (Garcia-Castro et al., 2002; Heeg-Truesdell and LaBonne, 2006; Steventon et al., 2009; Taneyhill and Bronner-Fraser, 2005; Wu et al., 2005). Tcf7l1 was able to significantly reduce the levels of Wnt reporter signal by competing with Tcf7 and Lef1 or by decreasing the pool of free ΔNβ-catenin required for transactivation by the Tcf/Lefs in the transient SuperTopFlash (STF) reporter assay in HEK293 cells (Fig. S3A). We therefore asked whether the expansion of NC cells in *AP2α-Cre;Tcf7l1*$^{fl/fl}$ mutants was caused by upregulation of Wnt/β-catenin signaling.

The expression of *Sp5* mRNA, a known Wnt/β-catenin target gene (Fujimura et al., 2007), was upregulated and expanded rostrally in the mutant embryos at the 6 s stage (Fig. 4A). Apart from its role in MHB formation (McMahon and Bradley, 1990; Thomas and Capecchi, 1990), Wnt1 is required during NC development (Ikeya et al., 1997; Saint-Jeannet et al., 1997). We found aberrant *Wnt1* mRNA expression in the ANF of *AP2α-Cre;Tcf7l1*$^{fl/fl}$ mutants at the 5-6 s stage (Fig. 4B). The ectopic pattern of *Wnt1* mRNA expression along the NPB of the prosencephalon was even more apparent at E9.0 in *Tcf7l1* conditional mutants (Fig. 4B), but we did not notice any changes in *Wnt1* expression in the MHB (Fig. S3B). As a result we conclude that the aberrant *Wnt1* signal in the ANF reflects the abnormal NC induction rather than altered A-P patterning.

The upregulation of the Wnt ligand (Wnt1) and Wnt target (Sp5) suggests an ectopic activation of Wnt/β-catenin signaling in the anterior neuroectoderm of *AP2α-Cre;Tcf7l1*$^{fl/fl}$ mutants. To confirm this, BAT-gal reporter mice were crossed with *Tcf7l1* conditional mutants and the resulting embryos were analyzed using anti-β-galactosidase and anti-Sox9 antibodies. As expected, the BAT-gal immunofluorescence expanded anteriorly in the *AP2α-Cre;Tcf7l1*$^{fl/fl}$ mutants when compared with controls at the 8 s stage (Fig. 4C,D). This was accompanied by many ectopic Sox9^{+} cells, which were clearly visible from a frontal view of the 8 s stage embryos (Fig. 4D). Also, wild-type embryos showed many cells co-expressing Sox9 and BAT-gal (Fig. S3C), indicating that Sox9 may be induced by Wnt/β-catenin signaling.

Our data suggest that transdifferentiation of the ANF into NC cells in *AP2α-Cre;Tcf7l1*$^{fl/fl}$ mutants results from aberrant activation of the Wnt/β-catenin pathway. To verify this by an alternative approach, we activated Wnt/β-catenin signaling using *β-cat*$^{Ex3fl/+}$ mice (Harada et al., 1999), in which a truncated, non-degradable form of β-catenin (encoded by *Ctnnb1*) is produced upon AP2α-Cre-mediated recombination. The *AP2α-Cre;β-cat*$^{Ex3fl/+}$ embryos exhibited neural tube closure defects and did not survive beyond E10.5. The crossing of the BAT-gal reporter into *AP2α-Cre;β-cat*$^{Ex3fl/+}$ mutants revealed strong Wnt reporter activation in most of the head ectoderm and along the anterior NPB (Fig. 4C,E). However, when compared with the BAT-gal signal in the *AP2α-Cre;Tcf7l1*$^{fl/fl}$ mutants, it was clear that the levels were much weaker in the ANF of the *AP2α-Cre;β-cat*$^{Ex3fl/+}$ embryos (Fig. 4D,E). Again, Sox9 immunofluorescence reflected the BAT-gal expansion in *AP2α-Cre;β-cat*$^{Ex3fl/+}$ mutants (Fig. 4E), but it did not reach the most anterior tip of the neuroectoderm, unlike in *Tcf7l1* mutants (Fig. 4D).

Next, we attempted to compare the expression of several targets of the Wnt/β-catenin signaling pathway and NC-related genes using qRT-PCR. We isolated mRNA from dissected heads of individual *AP2α-Cre;β-cat*$^{Ex3fl/+}$ (n=6) and *AP2α-Cre;Tcf7l1*$^{fl/fl}$ embryos (n=6) at the 6-12 s stage (Fig. S3D) and corresponding controls *β-cat*$^{Ex3fl/+}$ and *AP2α-Cre;Tcf7l1*$^{fl/+}$ (n=5, Fig. S3E), respectively. Significantly higher levels of *Lef1* (3.94-fold) and *Axin2* (2.62-fold) mRNA were expressed in the *β-cat*$^{Ex3fl/+}$ heads when compared with *AP2α-Cre;Tcf7l1*$^{fl/fl}$ heads, reflecting the overall wider activation of the BAT-gal reporter (Fig. S3D). However, there was no significant difference in *Sp5* expression between these mutants, presumably as *Sp5* is upregulated to a similar extent in both mutants. *AP2α-Cre;β-cat*$^{Ex3fl/+}$ did not display significant changes in the levels of *Sox10*, *Foxd3* and *Pax3* mRNA in comparison to *AP2α-Cre;Tcf7l1*$^{fl/fl}$ mutants. Interestingly, *Sox9* mRNA expression was decreased to 50.5% and *Tfap2a* to 43.5%, suggesting that the induction of NC in *AP2α-Cre;β-cat*$^{Ex3fl/+}$ was weaker than in *AP2α-Cre;Tcf7l1*$^{fl/fl}$ heads at E8.5.

The qRT-PCR analysis of whole heads obviously concealed changes in the spatial distribution of mRNA expression. To assess this, we employed whole-mount RNA *in situ* hybridization of *AP2α-Cre;β-cat*$^{Ex3fl/+}$ embryos. Levels of *Sox9* mRNA were increased and they expanded along the lateral border of the ANF in the *β-cat*$^{Ex3fl/+}$ mutants at the 9 s stage (Fig. S3F), similarly to the Sox9 immunofluorescence shown in Fig. 4E. *Sox10* mRNA levels appeared weaker and their distribution was more disperse than in the controls at 10 s stage (Fig. S3G). At E9.0, *Sox10* was aberrantly expressed in the head and along the dorsal part of the posterior trunk in *AP2α-Cre;β-cat*$^{Ex3fl/+}$ embryos (Fig. S3H). Overall expression of *Foxd3* mRNA was elevated in *β-cat*$^{Ex3fl/+}$ mutants at the 8 s stage (Fig. S3I), and at E9.5 in the region roughly corresponding to that of developing sensory nerves (Fig. S3I′).

In addition to the effects on the NC population, the strong overproduction of stabilized β-catenin in *AP2α-Cre;β-cat*$^{Ex3fl/+}$ mutants led to disorganization of the neural tissue and the non-neural ectoderm along the NPB. This was clearly visible from the expanded expression of *Fgf8* and *Gbx2* mRNA at E9.5 (Fig. S3J-K). Of note, the characteristic pattern of *Fgf8* and *Gbx2* expression in the MHB was maintained in *AP2α-Cre;β-cat*$^{Ex3fl/+}$ mutants (Fig. S3J′,K) but the expression of both genes was expanded posteriorly along the NPB.

Next, we assayed NC delamination by immunofluorescence of neuroepithelial cells marked with N-cadherin and migrating NC cells labeled with Sox9 antibody. The delamination of mouse NC cells starts around the 4 s stage (Lee et al., 2013). Transverse sections of control and *Tcf7l1* conditional mutant embryos at the 5 s stage revealed no difference in the onset of delamination of Sox9^{+} cells (Fig. 4F). One day later at E9.5, we observed only a thin layer

Development (2016) 143, 2206-2216 doi:10.1242/dev.132357

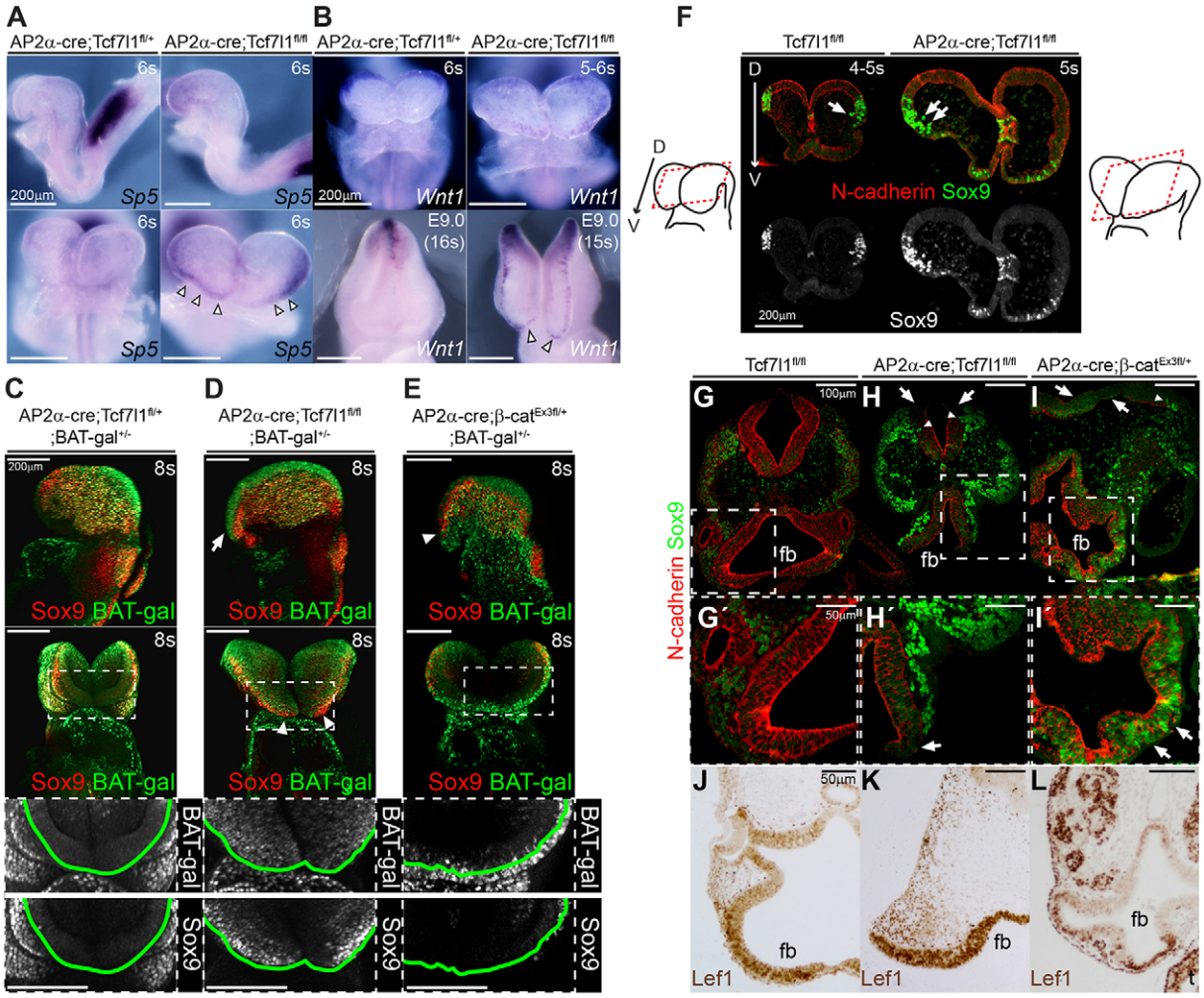

Fig. 4. Aberrant activation of Wnt signaling in *AP2α-Cre;Tcf7l1*$^{fl/fl}$ and *AP2α-Cre;β-cat*$^{Ex3fl/+}$ mutants. (A) *In situ* hybridization shows upregulation of the Wnt target *Sp5* along the NPB of the ANF in *AP2α-Cre;Tcf7l1*$^{fl/fl}$ mutants at 6 s stage (arrowheads). Side (top) and frontal (bottom) views. (B) Increase in expression of the Wnt ligand *Wnt1* along the NPB of the ANF in *AP2α-Cre;Tcf7l1*$^{fl/fl}$ mutants at 5-6 s and E9.0 stage (arrowheads). Frontal views. (C-E) BAT-gal signal (detected with β-galactosidase antibody; arrow) and Sox9 immunostaining (arrowheads) expand anteriorly in *AP2α-Cre;Tcf7l1*$^{fl/fl}$*;BAT-gal*$^{+/-}$ mutants at the 8 s stage (D). Both BAT-gal activation and ectopic Sox9 expansion are weaker in the neural ectoderm of *AP2α-Cre;β-cat*$^{Ex3fl/+}$*;BAT-gal*$^{+/-}$ mouse embryos at the same stage (E). Again, Sox9 immunofluorescence reflected the BAT-gal expansion in *AP2α-Cre;β-cat*$^{Ex3fl/+}$*;BAT-gal*$^{+/-}$ mutants (E, arrowhead). Green line demarcates the border between the neural and non-neural ectoderm. Note that BAT-gal signal was clearly activated in the most anterior non-neural ectoderm in the frontal view *AP2α-Cre;β-cat*$^{Ex3fl/+}$*;BAT-gal*$^{+/-}$. Side (top) and frontal (middle) views and higher magnification of the frontal views (boxed regions, black and white, bottom). (F) Transverse sections (as illustrated) of *AP2α-Cre;Tcf7l1*$^{fl/fl}$ and control embryos at 4-5 s stage stained for N-cadherin and Sox9. *Tcf7l1* conditional mutants showed no difference in the onset of delamination (arrows) at this stage. (G-I′) Transverse sections immunostained for N-cadherin and Sox9 at E9.5. The Sox9^{+} population is increased and N-cadherin staining is decreased in *AP2α-Cre;Tcf7l1*$^{fl/fl}$ and *AP2α-Cre;β-cat*$^{Ex3fl/+}$ mutants compared with controls. *Tcf7l1* conditional mutants with the strong phenotype display aberrant Sox9^{+} cells in the hindbrain prior to delamination (H, arrowheads) and N-cadherin expression is weaker in the anterior forebrain (H′, arrow) and in the dorsal hindbrain (H, arrows). Similarly, *AP2α-Cre;β-cat*$^{Ex3fl/+}$ embryos exhibit aberrant Sox9^{+} cells in the hindbrain (I, arrowheads), accompanied by substantial reduction in N-cadherin (I,I′, arrows). (J-L) Lef1 immunostaining of coronal sections of control (J), *AP2α-Cre;Tcf7l1*$^{fl/fl}$ (K) and *AP2α-Cre;β-cat*$^{Ex3fl/+}$ (L) embryos at E9.5. D, dorsal; V, ventral; fb, forebrain; t, tail. See also Fig. S3.

of Sox9^{+} cells between the N-cadherin^{+} forebrain tissue and the epidermis of control embryos. The hindbrain, labeled with N-cadherin, was found to be completely devoid of Sox9^{+} cells in the controls (Fig. 4G,G′). By contrast, *AP2α-Cre;Tcf7l1*$^{fl/fl}$ mutants clearly displayed aberrant Sox9^{+} cells in the hindbrain prior to delamination (Fig. 4H, Fig. S2C). Additionally, N-cadherin expression was weaker in the anterior forebrain (Fig. 4H′) and in the dorsal hindbrain (Fig. 4H) of the *Tcf7l1* conditional mutants with the strong phenotype. The same analysis of *AP2α-Cre;β-cat*$^{Ex3fl/+}$ embryos revealed that almost all forebrain cells converted into Sox9^{+} NC (Fig. 4I′). Similarly to *Tcf7l1* conditional mutants, we also detected aberrant Sox9-expressing cells in the hindbrain (Fig. 4I), accompanied by a massive decrease in the levels of N-cadherin (Fig. 4I,I′). Furthermore, protein levels of Lef1, a Wnt/β-catenin transcriptional activator and target gene (Galceran et al., 1999; Kratochwil et al., 2002; Liu et al., 2005), were increased in the forebrain of the *Tcf7l1* mutants compared with controls (Fig. 4J,K). *AP2α-Cre;β-cat*$^{Ex3fl/+}$ mutants also displayed very strong upregulation of Lef1 in the mesenchyme adjacent to the hindbrain as well as in the forebrain (Fig. 4J,L). The whole-mount immunofluorescence of wild-type embryos revealed colocalization of Lef1^{+} and Sox10^{+} cells at the 8 s stage (Fig. S3L).

Taken together, deletion of *Tcf7l1* resulted in ectopic activation of the Wnt/β-catenin pathway, suppression of neuroepithelial character and initiation of aberrant NC cell fate. Similar observations were made in conditional *AP2α-Cre;β-cat*$^{Ex3fl/+}$

Development (2016) 143, 2206-2216 doi:10.1242/dev.132357

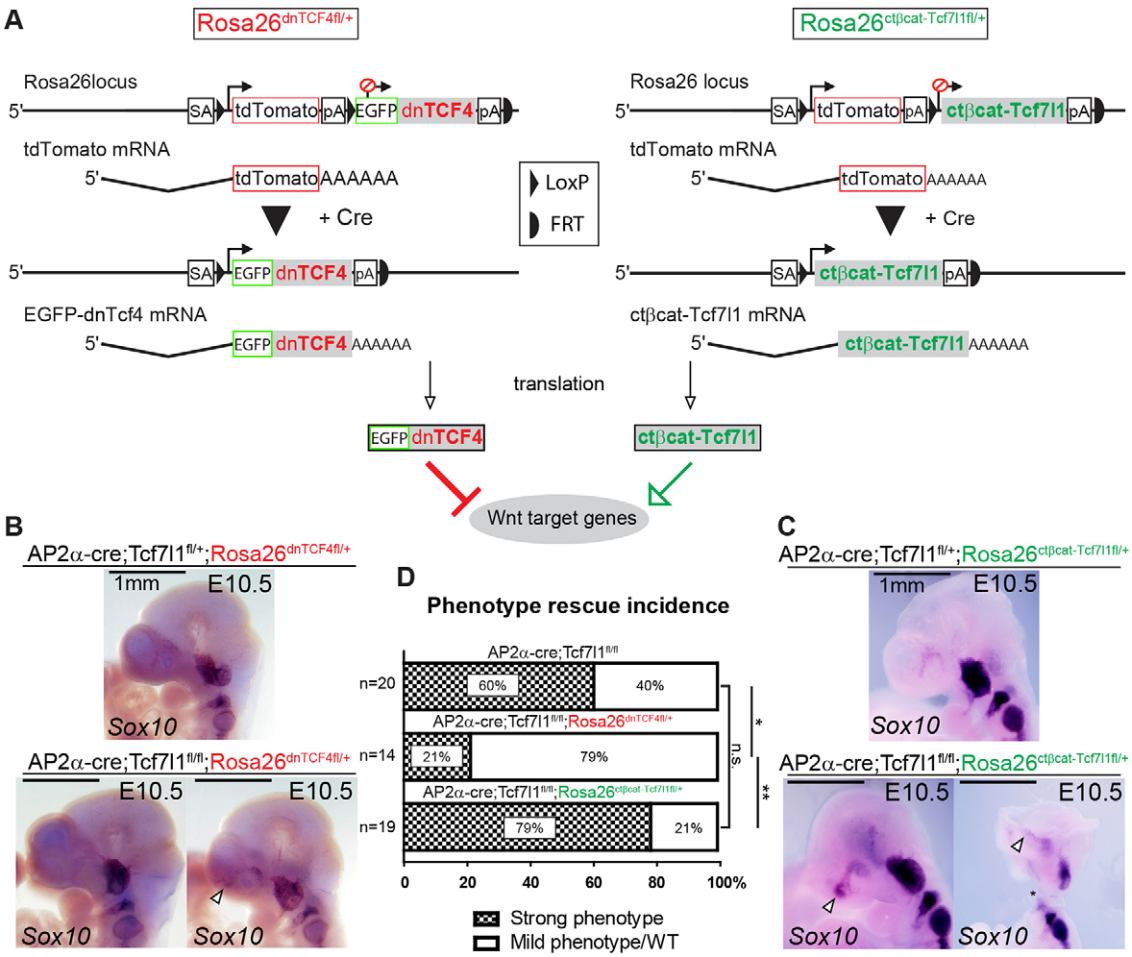

Fig. 5. The constitutive repressor dnTCF4 is able to rescue the ANF phenotype in *AP2α-Cre;Tcf7l1*$^{fl/fl}$ mutants. (A) Construction of the *Rosa26*$^{dnTCF4fl/+}$ and *Rosa26*$^{ctβcat\text{-}Tcf7l1fl/+}$ mouse strains used in the rescue experiments. SA, splice acceptor; pA, polyadenylation signal. (B) Expression of *Sox10* transcripts was either unaffected or only mildly affected in *AP2α-Cre;Tcf7l1*$^{fl/fl}$*;Rosa26*$^{dnTCF4fl/+}$ compound mutants, confirming the rescue capability of dnTCF4. (C) *AP2α-Cre;Tcf7l1*$^{fl/fl}$*;Rosa26*$^{ctβcat-Tcf7l1fl/+}$ compound mutants displayed no rescue, as confirmed by *Sox10 in situ* hybridization. Asterisk indicates an artifact caused during preparation. (D) Quantification of strong and mild phenotype incidence and rescue capability of dnTCF4 and ctβcat-Tcf7l1, scored at E10.5. **P*=0.0382, ***P*=0.0016, Fisher's exact test; n.s., not significant. *n*, number of embryos analyzed. See also Fig. S4.

mutants, although the onset of NC induction was delayed and less pronounced. Thus, the timing, spatial distribution and character of Wnt/β-catenin pathway activation differ slightly in the *AP2α-Cre;β-cat*$^{Ex3fl/+}$ and *Tcf7l1* conditional mutants.

The NC phenotype can be rescued with a truncated form of TCF7L2 but not with Tcf7l1 fused with β-catenin

Our data suggest that the loss of Tcf7l1-mediated repression of Wnt targets is the primary cause of NC cell fate expansion. In order to verify this hypothesis, we performed rescue experiments using two mouse strains conditionally expressing either dominant Tcf repressor or activator. As a dominant repressor we used the mouse strain *Rosa26*$^{dnTCF4fl/+}$, which contains the N-terminally truncated form of human TCF7L2 (dnTCF4) targeted into the *ROSA26* locus and inserted 3′ to the lox-STOP TdTomato (TdT) cassette (originally referred to as *Rosa26*$^{+/tdTomato}$) (Janeckova et al., 2016). This form cannot bind β-catenin and thus acts as a dominant repressor of Wnt/β-catenin targets. Second, we generated the mouse strain *Rosa26*$^{ctβcat\text{-}Tcf7l1fl/+}$, which allows conditional expression of full-length mouse Tcf7l1 fused with the transactivation domain of β-catenin (amino acids 696-781), analogous to the described Cat-Lef fusion (Hsu et al., 1998). This construct, which mimics β-catenin binding to Tcf7l1, was able to deliver mild activation of the Wnt reporter STF (Fig. S4A). Details of strain generation and characterization are presented in Fig. S4B-I. Following Cre recombination, the TdT cassette is excised, allowing production of either dnTCF4 or ctβcat-Tcf7l1 mRNA (Fig. 5A).

We crossed the *Tcf7l1*$^{fl/fl}$*;Rosa26*$^{dnTCF4fl/fl}$ and *AP2α-Cre;Tcf7l1*$^{fl/+}$ strains and evaluated the strength of the phenotype in *AP2α-Cre;Tcf7l1*$^{fl/fl}$*;Rosa26*$^{dnTCF4fl/+}$ compound mutants at E10.5. Overexpression of dnTCF4 was able to reduce the occurrence of the strong phenotype by more than half (to 21%), compared with the 60% incidence in *AP2α-Cre;Tcf7l1*$^{fl/fl}$ littermates (*P*=0.049, Fisher's exact test). The effect of the rescue on the NC population was further analyzed by *in situ* hybridization, showing no or very little ectopic *Sox10* mRNA in the *AP2α-Cre;Tcf7l1*$^{fl/fl}$*; Rosa26*$^{dnTCF4fl/+}$ 'rescued' mutants (Fig. 5B,D). By contrast, the βcat-Tcf7l1 fusion protein showed a significantly (*P*=0.0016, Fisher's exact test) decreased capability to rescue the phenotype compared with dnTCF4, as demonstrated by 79% of analyzed embryos displaying the strong phenotype in *AP2α-Cre;Tcf7l1*$^{fl/fl}$*; Rosa26*$^{ctβcat\text{-}Tcf7l1fl/+}$ compound mutants. Expression of ctβcat-Tcf7l1 was also unable to reduce the aberrant *Sox10*$^{+}$ NC population (Fig. 5C,D). In summary, using transgenic mouse

Development (2016) 143, 2206-2216 doi:10.1242/dev.132357

strains, we genetically confirmed that Tcf7l1, acting as a repressor of Wnt/β-catenin signaling, protects the anterior neural tissue from conversion to the NC cell fate.

DISCUSSION

Progressive activation of the Wnt/β-catenin pathway affects the development of anterior neural tissue and NC

Spatiotemporal regulation of Wnt/β-catenin pathway activation, which is required for proper development of the prosencephalon, is secured by the expression of several ANF-specific negative regulators of Wnt/β-catenin signaling. Our data, together with evidence from others (Cole et al., 2008; Liu et al., 2005; Ombrato et al., 2012; Wu et al., 2012), characterize Tcf7l1 as a repressor of Wnt/β-catenin target genes. Aberrant activation of the Wnt/β-catenin pathway in *Tcf7l1* systemic mutants is regarded as the cause of strong A-P patterning defects both in zebrafish (Dorsky et al., 2003; Kim et al., 2000) and mouse (Merrill et al., 2004). *tcf7l1a* loss-of-function (*hdl*) zebrafish mutants or *tcf7l1a* and *tcf7l1b* morphants display a shift in the expression of the MHB markers *pax2.1* and *gbx1* towards the anterior, which is accompanied by the loss of *six3* and *rx3* expression (Dorsky et al., 2003). The *Tcf7l1* mouse systemic mutants also display expansion of the midbrain marker *En1* and downregulation of *Hesx1* (Merrill et al., 2004). Similarly, deletion of *Dkk1* (Mukhopadhyay et al., 2001), *Six3* (Lagutin et al., 2003), *Hesx1* (Andoniadou et al., 2007) and *ICAT* (*Ctnnbip1*) (Satoh et al., 2004) in mouse is followed by the loss of anterior neural tissue. This has usually been interpreted as a defect in A-P patterning induced by aberrant Wnt/β-catenin signaling. We think that this is a simplified view and that, in the context of the ANF phenotypes, it is only partially true. In *Xenopus*, low levels of ectopic Wnt/β-catenin activation enrich the NC population without affecting A-P patterning, whereas high doses affect both (Wu et al., 2005). This scenario might be also valid for mammals because mice carrying ENU-induced activating point mutations in Lrp6 and β-catenin display a gradual loss of the prospective prosencephalon depending on the strength of the Wnt/β-catenin pathway overactivation, but they do not manifest an anterior shift of posterior neural markers (Fossat et al., 2011). Furthermore, compound deletion of one *Hesx1* allele and both alleles of *Tcf7l1* in mouse, using prosencephalon-specific *Hesx1-Cre*, results in the aberrant activation of Wnt/β-catenin signaling that leads to a loss of anterior neural tissue, whereas A-P patterning remains unchanged (Andoniadou et al., 2011). Our observations in *AP2α-Cre;Tcf7l1*$^{fl/fl}$ mutants are in agreement with these data as we did not detect any alteration in expression of *Fgf8* or *Gbx2* in the MHB (Fig. 2). Nevertheless, we did observe a gradual loss of the ANF markers *Six3*, *Fgf8* and *Foxg1* and the posterior prosencephalon marker *Tcf7l2* depending on the strength of the phenotype. This was accompanied by enrichment of the *Tfap2a*$^{+}$, *Pax3*$^{+}$, *Sox9*$^{+}$, *Foxd3*$^{+}$ and *Sox10*$^{+}$ NC population and its expansion along the lateral border of the anterior ANF (Fig. 3). We therefore provide a new explanation for the loss of the ANF. The absence of Tcf7l1-mediated repression of Wnt target genes in *AP2α-Cre;Tcf7l1*$^{fl/fl}$ mutants allows the gradient of Wnt ligands to influence cell fate in a wider region of the ANF than normally. This permits NC induction in the ANF, while A-P patterning of the neural tissue remains unaltered. A different experimental design, based on Wnt/β-catenin pathway overactivation in *AP2α-Cre;β-cat*$^{Ex3fl/+}$ mutants, also resulted in aberrant NC induction that was spread along the A-P axis. In contrast to *AP2α-Cre;Tcf7l1*$^{fl/fl}$ mutants, the most anterior neural fold did not convert to NC in *AP2α-Cre;β-cat*$^{Ex3fl/+}$ mutants (Fig. 4, Fig. S3). This might be explained by a lower activation of the Wnt/β-catenin pathway in the ANF of *AP2α-Cre;β-cat*$^{Ex3fl/+}$ than of *AP2α-Cre;Tcf7l1*$^{fl/fl}$ mutants, as judged by the BAT-gal reporter (Fig. 4). We think that the presence of several factors, including Tcf7l1, antagonizing Wnt-induced transcription in the ANF may attenuate the effect of stabilized β-catenin.

The timing of Wnt/β-catenin activation in the head neuroectoderm is crucial. It has been shown in *Xenopus* that NPB loses its competence for NC induction by Wnts with time due to increasing BMP activity (Steventon et al., 2009; Steventon and Mayor, 2012). The use of *AP2α-Cre* (onset of Cre recombination prior to neurulation, later expressed along the NPB) instead of the widely used *Wnt1-Cre* (onset of Cre recombination around the 5 s stage, expressed in already specified NC) (Danielian et al., 1998; Lewis et al., 2013) can yield dramatically different NC phenotypes. In *AP2α-Cre;β-cat*$^{Ex3fl/+}$ mutants, we affected the population of undifferentiated Sox9^{+} and *Foxd3*-expressing NC cells as early as at the 8 s stage, whereas in *Wnt1-Cre/β-cat*$^{Ex3fl/+}$ mutants altered NC differentiation was observed much later at E10.5 (Lee et al., 2004). This indicates the *AP2α-Cre* driver to be a more suitable tool for studying early events of NC development. Our data provide evidence for an earlier role of the Wnt/β-catenin pathway in NC development than evident from previously published findings in the mouse model showing the requirement for the Wnt/β-catenin pathway in NC maintenance and differentiation (Brault et al., 2001; Gay et al., 2015; Lee et al., 2004).

The effects of the Tcf7l1 deficiency in mice and zebrafish on NC development were not, until now, characterized in detail. Analogous to the NC expansion in *AP2α-Cre;Tcf7l1*$^{fl/fl}$ mice (Figs 3,4, Fig. S2), we observed ectopic expression of *foxd3*, *pax3* and *sox9* mRNA along the entire anterior NPB of *tcf7l1a/b* morphants in zebrafish. Our rescue experiments with co-injection of mouse *Tcf7l1* mRNA implicate the conservation of Tcf7l1 function across vertebrate species. In accordance, MO-mediated knockdown of Dkk1 in *Xenopus* is followed by enrichment of the NC population, which is marked by the expansion of *Snail2* towards the anterior portion of the embryo (Carmona-Fontaine et al., 2007). In mouse, loss of Dkk1 has been shown to cause expansion of the NC marker *Sox10* anteriorly (Carmona-Fontaine et al., 2007). Similarly, *Hesx1* mutant mice display expansion of Wnt target genes together with the NC markers *Pax3* and *Foxd3* towards the anterior (Andoniadou et al., 2007). Mutual functional redundancy of these factors was demonstrated in zebrafish in which injection of either *Six3* or *Hesx1* mRNA rescued the *hdl* phenotype (*tcf7l1a* deletion) (Andoniadou et al., 2011; Lagutin et al., 2003). All these data are in agreement with the interpretation of *Tcf7l1* mutants presented here.

In summary, collective evidence points towards the coordinated expression of several Wnt/β-catenin pathway inhibitors in the anterior neuroectoderm that together define, under physiological conditions, a spatial border to the expansion of the NC. Similarity in the phenotypes following their deficiency suggests that the ANF region is very close to the threshold of Wnt/β-catenin activation for NC induction. Therefore, from the evolutionary perspective, attenuation of the sensitivity to Wnt/β-catenin signaling in the ANF region by fine-tuning the expression levels of Wnt signaling inhibitors might represent a very sensitive tool that allows the simultaneous modification of two prominent vertebrate features, namely the NC and the forebrain.

A key question remains: which Wnt/β-catenin target genes act as NC inducers?

Our analysis of *AP2α-Cre;Tcf7l1*$^{fl/fl}$ mutants identified Tcf7l1 as a negative regulator of the NC population. Given that the NC is

Development (2016) 143, 2206-2216 doi:10.1242/dev.132357

positively regulated by the Wnt/β-catenin pathway in all vertebrates studied, other Tcf/Lefs should be responsible for activation of Wnt/β-catenin targets in the NC. It is likely that Lef1, Tcf7 and Tcf7l2 are redundant in NC cells, since whole-body double knockouts of *Lef1/Tcf7* and *Tcf7/Tcf7l2* in mice do not display any obvious NC phenotype (Galceran et al., 1999; Gregorieff et al., 2004). Ectopic $Sox9^{+}$ cells in *AP2α-Cre;β-cat*$^{Ex3fl/+}$ mutants spatially overlap with the elevation of the BAT-gal reporter, Lef1 and Tcf7, but not Tcf7l2 proteins (Fig. 4; data not shown), suggesting that Lef1 and Tcf7 are positively regulated by Wnt/β-catenin signaling and probably participate in the expression of Wnt-responsive NC-specific genes. In *Xenopus*, Tfap2α is both required and sufficient for induction of NC. Additionally, expression of *Tfap2a* was inhibited by injection of an MO against β-catenin at stage 17 (de Croze et al., 2011), raising the possibility that *Tfap2a* is a Wnt/β-catenin target gene. This is in agreement with the data presented here showing upregulation of Tfap2α expression in *AP2α-Cre;Tcf7l1*$^{fl/fl}$ mutants (Fig. 3). Sp5, another well-defined Wnt target gene and transcriptional repressor (Fujimura et al., 2007), was strongly upregulated in *AP2α-Cre;Tcf7l1*$^{fl/fl}$ mutants, spreading its expression across the entire ANF (Fig. 4). The work in *Xenopus* has identified Sp5 as a novel NC-specific inducer (Park et al., 2013). MO-mediated knockdown of Sp5 leads to the upregulation of *Zic1*, making it a candidate target of Sp5 repression. Zic1 is able to initiate NC formation only when expressed in appropriate balance with Pax3, another NC inducer (Hong and Saint-Jeannet, 2007; Park et al., 2013). *Pax3*, which is also upregulated in *AP2α-Cre;Tcf7l1* mutants (Fig. 3), has recently been identified as a direct target of Tcf/Lefs (Zhao et al., 2014), providing an additional link to the gene regulatory network driving NC induction. Aberrant induction of Sp5-mediated repression of *Zic1*, in combination with the ectopic expression of Wnt1 ligand (Fig. 4), which enhances the β-catenin/Tcf/Lef-driven transcription of *Pax3*, might serve as an artificial positive-feedback loop, further potentiating the effects on NC induction. Additionally, the aberrant Wnt/β-catenin signaling present in *AP2α-Cre;Tcf7l1*$^{fl/fl}$ mutants might upregulate the expression of *Axud1* (*Csrnp1*), a novel Wnt-dependent positive regulator of NC specification (Simões-Costa et al., 2015).

In summary, we have demonstrated that Tcf7l1-mediated repression of β-catenin target genes protects the anterior neuroectoderm from converting into NC. Thereby, we (1) help to eliminate the ambiguity in the interpretation of NC development in mouse and other vertebrate model organisms and (2) provide a model explaining the phenotypes previously acquired in mouse following derepression of the Wnt/β-catenin signaling pathway during early brain development.

MATERIALS AND METHODS

Mouse strains

Housing of mice and *in vivo* experiments were performed in compliance with the European Communities Council Directive of 24 November 1986 (86/609/EEC) and national and institutional guidelines. All procedures involving experimental animals were approved by the Institutional Committee for Animal Care and Use (permission PP-071/2011, PP-281/2011).

AP2α-IRESCre (*AP2α-Cre*) was described previously (Macatee et al., 2003). Cre reporter lines *Rosa26*$^{EYFPfl/+}$ [B6.129X1-*Gt(ROSA)26Sor*$^{tm1(EYFP)Cos}$/J, stock no. 00614] and *ROSA26* [B6.129S4-*Gt(ROSA)26Sor*^{tm1Sor}/J, stock no. 003474] were purchased from The Jackson Laboratory. *Tcf7l1*$^{fl/+}$ strain [*Tcf7l1*$^{tm1a(EUCOMM)Wtsi}$] was purchased from the EUCOMM. Transgenic mouse strain BAT-gal (Maretto et al., 2003) was kindly provided by S. Piccolo. Mice with a conditional 'floxed' β-catenin (floxed *Ctnnb1* exon 3, referred to as *β-cat*$^{Ex3fl/+}$) were provided by M.M.T. (Harada et al., 1999). Generation of *Rosa26*$^{dnTCF4fl/+}$ was described by Janeckova et al. (2016). Briefly, human TCF7L2 coding sequence lacking the N-terminal domain (amino acids 1-31) was cloned into the *ROSA26* targeting vector, which contains arms for homologous recombination into the *ROSA26* locus, in the same way as when generating *Rosa26*$^{ctβcat\text{-}Tcf7l1fl/+}$. Details of *Rosa26*$^{ctβcat\text{-}Tcf7l1fl/+}$ mouse line generation are provided in Fig. S4. A C-terminal part of β-catenin (amino acids 696-781) was fused with mouse full-length Tcf7l1 and inserted into the *ROSA26* locus by homologous recombination in R1 embryonic stem cells (Stem Cell Technologies). The construct carries tdTomato (kindly provided by Roger Tsian, UC San Diego, CA, USA) coding sequence flanked by LoxP sites serving as a stop cassette for ctβcat-Tcf7l1. Excision of the tdTomato cassette via Cre-mediated recombination allows transcription of ctβcat-Tcf7l1 mRNA (Fig. 5A). The PGK-Neo cassette was removed by crossing F1 animals with the *Actb:FLPe* mouse strain expressing FLP-FRT recombinase (Rodríguez et al., 2000), backcrossed with C57BL/6J for six generations. All above-mentioned mouse strains were kept on a C57BL/6J background.

Primers (5′-3′) for genotyping the *Rosa26*$^{ctβcat\text{-}Tcf7l1fl/+}$ allele: JM21F, GAGGAGCCATAACTGCAGAC; JM23R, CCTGGCTATCCTAGATAGAAC; and JM27R, GTACTGTTCCACGATGGT. The expected size of the PCR product is 965 bp in the mutant and 300 bp in the wild type. Recombination in *AP2α-Cre;Tcf7l1*$^{fl/fl}$*;Rosa26*$^{ctβcat\text{-}Tcf7l1fl/+}$ was detected using a mix of JM21F, JM27R and JM05B GATCAGCTCGTCGTTCGCTC primers, resulting in PCR products of 970 bp prior to, and 777 bp after, recombination.

MO knockdown in zebrafish

Zebrafish wild-type, single-cell embryos were injected with a combination of previously described *tcf7l1a* (5′-CTCCGTTTAACTGAGGCATGTTGGC-3′) and *tcf7l1b* (5′-CGCCTCCGTTAAGCTGCGGCATGTT-3′) MOs (Dorsky et al., 2003) (Gene Tools) in a 1:1 ratio at a final concentration of 1.6 ng/nl (1-2 nl injected). Mouse *Tcf7l1* mRNA used in rescue experiments was synthesized using the mMESSAGE mMACHINE Kit (Ambion) and 10 pg was injected. Embryos were raised at 28°C and harvested at 12 hpf.

Immunohistochemistry and RNA *in situ* hybridization

At least three embryos of each genotype and similar developmental stage were analyzed per staining. Primary antibodies are listed in Table S1. Secondary antibodies were anti-mouse, anti-chicken, anti-rabbit or anti-goat Alexa Fluor 488 or 594 (1:500; Life Technologies) and biotinylated anti-rabbit (1:500; Vector Laboratories), with the Vectastain ABC Elite Kit and ImPACT DAB substrate (all Vector Laboratories). For whole-mount immunohistochemistry we used the protocol of Sandell et al. (2014). Briefly, embryos were fixed overnight in 4% paraformaldehyde (PFA), permeabilized using Dent's bleach and 100% methanol and rehydrated. Blocking for 2 h and antibody incubation overnight were performed in 3% BSA in 0.1 M Tris-Cl pH 7.5, 0.15 M NaCl, 0.03% Triton X-100. Washing five times for 1 h each in PBS was followed by overnight incubation with secondary antibody in the blocking buffer. The next day, embryos were stained for nuclei using Hoechst (1:1000; Life Technologies), washed three times in PBS (20 min each) and stored in 2% formaldehyde (Sigma). Whole-mount immunofluorescence was captured using an Apotome.2 Ax10 zoom.V16 (Zeiss) binocular microscope. Fluorescence and brightfield light images were acquired with a Nikon Diaphot 300 with 4×/0.1 NA and 10×/0.25 NA objectives and a Leica SP5 confocal microscope.

Whole-mount *in situ* hybridization was performed using standard protocols. Riboprobes were cloned into pGEM-T-Easy vector (Promega) using the primers specified in Table S1.

SuperTopFlash reporter assay

HEK293 cells (30,000 cells/well of a 96-well plate) were transiently transfected using Lipofectamine 2000 (Invitrogen) with 30 ng Super8X TopFlash (kind gift from Randall Moon) and 1 ng Renilla luciferase constructs and the indicated amount of expression vector, supplemented with carrier DNA to a total final concentration of 200 ng DNA per well. Luciferase assays were performed 48 h later with a Dual-Glo Luciferase Kit (Promega). The luciferase signal was normalized to the co-transfected Renilla readout. Experiments were repeated at least three times, using biological replicates.

Development (2016) 143, 2206-2216 doi:10.1242/dev.132357

Quantitative real-time (qRT) PCR

To analyze mRNA expression in *AP2α-Cre;β-cat*$^{Ex3fl/+}$ and *AP2α-Cre; Tcf7l1*$^{fl/fl}$ heads, eyes from 6-12 s stage (E8.5) mouse embryos were dissected and total RNA was isolated with Trizol Reagent (Life Technologies). Random-primed cDNA was generated from 200 ng total RNA using the SuperScript VILO cDNA Synthesis Kit (Life Technologies). Six different embryos originating from three litters were used for tissue dissection and subsequent analysis per genotype. qRT-PCR reactions were run in a LightCycler 480 instrument (Roche) using a 5 µl reaction mixture of DNA and SYBR Green I Master (Roche). Analysis was performed on replicates of six individual samples per genotype, run in duplicate. The average Cp values of all biological and technical replicates were normalized to endogenous levels of *Tbp*. Statistical significance of the change in mRNA expression was calculated by a two-tailed Student's *t*-test. Change in mRNA expression was presented as the ratio of *AP2α-Cre;β-cat*$^{Ex3fl/+}$ to *AP2α-Cre; Tcf7l1*$^{fl/fl}$ on a $\log_2$ scale. Primer sequences are listed in Table S1.

Acknowledgements

We thank K. Kovacova, J. Lachova, L. Svobodova and V. Noskova for excellent technical support; F. Dupacova for help with paraffin sectioning; and S. Piccolo for providing BAT-gal.

Competing interests

The authors declare no competing or financial interests.

Author contributions

J.M., O.M. and Z.K. conceived and designed the experimental approach. V.K. and M.M.T. provided new analytic tools. J.M. and O.M. performed the experiments and analyzed the data. J.M., O.M. and Z.K. wrote the manuscript.

Funding

This work was supported by the Grant Agency of the Czech Republic (Grantová Agentura České Republiky) [P305/12/2042 to O.M., GACR 14-33952S to V.K.]; Ministry of Education, Youth and Sports of the Czech Republic (Ministerstvo Školství, Mládeže a Tělovýchovy) [LK11214 to O.M., LO1419 to Z.K.]; the Grant Agency of Charles University (Univerzita Karlova) [GAUK-521212 to J.M.]; and by BIOCEV – Biotechnology and Biomedicine Centre of the Academy of Sciences and Charles University (Biotechnologické a Biomedicínské Centrum Akademie věd a Univerzity Karlovy ve Vestci) [CZ.1.05/1.1.00/02.0109 and RVO68378050 to Z.K.].

Supplementary information

Supplementary information available online at
http://dev.biologists.org/lookup/suppl/doi:10.1242/dev.132357/-/DC1

References

Andoniadou, C. L., Signore, M., Sajedi, E., Gaston-Massuet, C., Kelberman, D., Burns, A. J., Itasaki, N., Dattani, M. and Martinez-Barbera, J. P. (2007). Lack of the murine homeobox gene Hesx1 leads to a posterior transformation of the anterior forebrain. *Development* **134**, 1499-1508.

Andoniadou, C. L., Signore, M., Young, R. M., Gaston-Massuet, C., Wilson, S. W., Fuchs, E. and Martinez-Barbera, J. P. (2011). HESX1- and TCF3-mediated repression of Wnt/beta-catenin targets is required for normal development of the anterior forebrain. *Development* **138**, 4931-4942.

Bang, A. G., Papalopulu, N., Goulding, M. D. and Kintner, C. (1999). Expression of Pax-3 in the lateral neural plate is dependent on a Wnt-mediated signal from posterior nonaxial mesoderm. *Dev. Biol.* **212**, 366-380.

Barriga, E. H., Trainor, P. A., Bronner, M. and Mayor, R. (2015). Animal models for studying neural crest development: is the mouse different? *Development* **142**, 1555-1560.

Brault, V., Moore, R., Kutsch, S., Ishibashi, M., Rowitch, D. H., McMahon, A. P., Sommer, L., Boussadia, O. and Kemler, R. (2001). Inactivation of the beta-catenin gene by Wnt1-Cre-mediated deletion results in dramatic brain malformation and failure of craniofacial development. *Development* **128**, 1253-1264.

Burstyn-Cohen, T., Stanleigh, J., Sela-Donenfeld, D. and Kalcheim, C. (2004). Canonical Wnt activity regulates trunk neural crest delamination linking BMP/noggin signaling with G1/S transition. *Development* **131**, 5327-5339.

Cadigan, K. M. and Waterman, M. L. (2012). TCF/LEFs and Wnt signaling in the nucleus. *Cold Spring Harb. Perspect. Biol.* **4**, a007906.

Carmona-Fontaine, C., Acuña, G., Ellwanger, K., Niehrs, C. and Mayor, R. (2007). Neural crests are actively precluded from the anterior neural fold by a novel inhibitory mechanism dependent on Dickkopf1 secreted by the prechordal mesoderm. *Dev. Biol.* **309**, 208-221.

Castrop, J., van Norren, K. and Clevers, H. (1992). A gene family of HMG-box transcription factors with homology to TCF-1. *Nucleic Acids Res.* **20**, 611.

Cheung, M. and Briscoe, J. (2003). Neural crest development is regulated by the transcription factor Sox9. *Development* **130**, 5681-5693.

Cheung, M., Chaboissier, M.-C., Mynett, A., Hirst, E., Schedl, A. and Briscoe, J. (2005). The transcriptional control of trunk neural crest induction, survival, and delamination. *Dev. Cell* **8**, 179-192.

Clevers, H. and Nusse, R. (2012). Wnt/beta-catenin signaling and disease. *Cell* **149**, 1192-1205.

Cole, M. F., Johnstone, S. E., Newman, J. J., Kagey, M. H. and Young, R. A. (2008). Tcf3 is an integral component of the core regulatory circuitry of embryonic stem cells. *Genes Dev.* **22**, 746-755.

Danielian, P. S., Muccino, D., Rowitch, D. H., Michael, S. K. and McMahon, A. P. (1998). Modification of gene activity in mouse embryos in utero by a tamoxifen-inducible form of Cre recombinase. *Curr. Biol.* **8**, 1323-1326.

de Croze, N., Maczkowiak, F. and Monsoro-Burq, A. H. (2011). Reiterative AP2a activity controls sequential steps in the neural crest gene regulatory network. *Proc. Natl. Acad. Sci. USA* **108**, 155-160.

Dorsky, R. I., Itoh, M., Moon, R. T. and Chitnis, A. (2003). Two tcf3 genes cooperate to pattern the zebrafish brain. *Development* **130**, 1937-1947.

Dottori, M., Gross, M. K., Labosky, P. and Goulding, M. (2001). The winged-helix transcription factor Foxd3 suppresses interneuron differentiation and promotes neural crest cell fate. *Development* **128**, 4127-4138.

Fossat, N., Jones, V., Khoo, P.-L., Bogani, D., Hardy, A., Steiner, K., Mukhopadhyay, M., Westphal, H., Nolan, P. M., Arkell, R. et al. (2011). Stringent requirement of a proper level of canonical WNT signalling activity for head formation in mouse embryo. *Development* **138**, 667-676.

Fujimura, N., Vacik, T., Machon, O., Vlcek, C., Scalabrin, S., Speth, M., Diep, D., Krauss, S. and Kozmik, Z. (2007). Wnt-mediated down-regulation of Sp1 target genes by a transcriptional repressor Sp5. *J. Biol. Chem.* **282**, 1225-1237.

Galceran, J., Farinas, I., Depew, M. J., Clevers, H. and Grosschedl, R. (1999). Wnt3a-/–like phenotype and limb deficiency in Lef1(-/-)Tcf1(-/-) mice. *Genes Dev.* **13**, 709-717.

Garcia-Castro, M. I., Marcelle, C. and Bronner-Fraser, M. (2002). Ectodermal Wnt function as a neural crest inducer. *Science* **297**, 848-851.

Garnett, A. T., Square, T. A. and Medeiros, D. M. (2012). BMP, Wnt and FGF signals are integrated through evolutionarily conserved enhancers to achieve robust expression of Pax3 and Zic genes at the zebrafish neural plate border. *Development* **139**, 4220-4231.

Gay, M. H.-P., Valenta, T., Herr, P., Paratore-Hari, L., Basler, K. and Sommer, L. (2015). Distinct adhesion-independent functions of beta-catenin control stage-specific sensory neurogenesis and proliferation. *BMC Biol.* **13**, 24.

Gregorieff, A., Grosschedl, R. and Clevers, H. (2004). Hindgut defects and transformation of the gastro-intestinal tract in Tcf4(-/-)/Tcf1(-/-) embryos. *EMBO J.* **23**, 1825-1833.

Groves, A. K. and LaBonne, C. (2014). Setting appropriate boundaries: fate, patterning and competence at the neural plate border. *Dev. Biol.* **389**, 2-12.

Hanashima, C., Li, S. C., Shen, L., Lai, E. and Fishell, G. (2004). Foxg1 suppresses early cortical cell fate. *Science* **303**, 56-59.

Harada, N., Tamai, Y., Ishikawa, T.-o., Sauer, B., Takaku, K., Oshima, M. and Taketo, M. M. (1999). Intestinal polyposis in mice with a dominant stable mutation of the beta-catenin gene. *EMBO J.* **18**, 5931-5942.

Heeg-Truesdell, E. and LaBonne, C. (2006). Neural induction in Xenopus requires inhibition of Wnt-beta-catenin signaling. *Dev. Biol.* **298**, 71-86.

Hong, C.-S. and Saint-Jeannet, J.-P. (2007). The activity of Pax3 and Zic1 regulates three distinct cell fates at the neural plate border. *Mol. Biol. Cell* **18**, 2192-2202.

Hsu, S.-C., Galceran, J. and Grosschedl, R. (1998). Modulation of transcriptional regulation by LEF-1 in response to Wnt-1 signaling and association with beta-catenin. *Mol. Cell. Biol.* **18**, 4807-4818.

Ikeya, M., Lee, S. M., Johnson, J. E., McMahon, A. P. and Takada, S. (1997). Wnt signalling required for expansion of neural crest and CNS progenitors. *Nature* **389**, 966-970.

Janeckova, L., Fafilek, B., Krausova, M., Horazna, M., Vojtechova, M., Alberich-Jorda, M., Sloncova, E., Galuskova, K., Sedlacek, R., Anderova, M. et al. (2016). Wnt signaling inhibition deprives small intestinal stem cells of clonogenic capacity. *Genesis* **54**, 101-114.

Janssens, S., Van Den Broek, O., Davenport, I. R., Akkers, R. C., Liu, F., Veenstra, G. J. C., Hoppler, S., Vleminckx, K. and Destrée, O. (2013). The Wnt signaling mediator tcf1 is required for expression of foxd3 during Xenopus gastrulation. *Int. J. Dev. Biol.* **57**, 49-54.

Kim, C.-H., Oda, T., Itoh, M., Jiang, D., Artinger, K. B., Chandrasekharappa, S. C., Driever, W. and Chitnis, A. B. (2000). Repressor activity of Headless/Tcf3 is essential for vertebrate head formation. *Nature* **407**, 913-916.

Kléber, M., Lee, H.-Y., Wurdak, H., Buchstaller, J., Riccomagno, M. M., Ittner, L. M., Suter, U., Epstein, D. J. and Sommer, L. (2005). Neural crest stem cell maintenance by combinatorial Wnt and BMP signaling. *J. Cell Biol.* **169**, 309-320.

Korinek, V., Barker, N., Willert, K., Molenaar, M., Roose, J., Wagenaar, G., Markman, M., Lamers, W., Destree, O. and Clevers, H. (1998). Two members of

the Tcf family implicated in Wnt/beta-catenin signaling during embryogenesis in the mouse. *Mol. Cell. Biol.* **18**, 1248-1256.
Kratochwil, K., Galceran, J., Tontsch, S., Roth, W. and Grosschedl, R. (2002). FGF4, a direct target of LEF1 and Wnt signaling, can rescue the arrest of tooth organogenesis in Lef1(-/-) mice. *Genes Dev.* **16**, 3173-3185.
Lagutin, O. V., Zhu, C. C., Kobayashi, D., Topczewski, J., Shimamura, K., Puelles, L., Russell, H. R. C., McKinnon, P. J., Solnica-Krezel, L. and Oliver, G. (2003). Six3 repression of Wnt signaling in the anterior neuroectoderm is essential for vertebrate forebrain development. *Genes Dev.* **17**, 368-379.
Lee, H.-Y., Kleber, M., Hari, L., Brault, V., Suter, U., Taketo, M. M., Kemler, R. and Sommer, L. (2004). Instructive role of Wnt/beta-catenin in sensory fate specification in neural crest stem cells. *Science* **303**, 1020-1023.
Lee, R. T. H., Nagai, H., Nakaya, Y., Sheng, G., Trainor, P. A., Weston, J. A. and Thiery, J. P. (2013). Cell delamination in the mesencephalic neural fold and its implication for the origin of ectomesenchyme. *Development* **140**, 4890-4902.
Lewis, A. E., Vasudevan, H. N., O'Neill, A. K., Soriano, P. and Bush, J. O. (2013). The widely used Wnt1-Cre transgene causes developmental phenotypes by ectopic activation of Wnt signaling. *Dev. Biol.* **379**, 229-234.
Li, B., Kuriyama, S., Moreno, M. and Mayor, R. (2009). The posteriorizing gene Gbx2 is a direct target of Wnt signalling and the earliest factor in neural crest induction. *Development* **136**, 3267-3278.
Litsiou, A., Hanson, S. and Streit, A. (2005). A balance of FGF, BMP and WNT signalling positions the future placode territory in the head. *Development* **132**, 4051-4062.
Liu, F., van den Broek, O., Destrée, O. and Hoppler, S. (2005). Distinct roles for Xenopus Tcf/Lef genes in mediating specific responses to Wnt/beta-catenin signalling in mesoderm development. *Development* **132**, 5375-5385.
Liu, J. A. J., Wu, M.-H., Yan, C. H., Chau, B. K. H., So, H., Ng, A., Chan, A., Cheah, K. S. E., Briscoe, J. and Cheung, M. (2013). Phosphorylation of Sox9 is required for neural crest delamination and is regulated downstream of BMP and canonical Wnt signaling. *Proc. Natl. Acad. Sci. USA* **110**, 2882-2887.
Macatee, T. L., Hammond, B. P., Arenkiel, B. R., Francis, L., Frank, D. U. and Moon, A. M. (2003). Ablation of specific expression domains reveals discrete functions of ectoderm- and endoderm-derived FGF8 during cardiovascular and pharyngeal development. *Development* **130**, 6361-6374.
Maretto, S., Cordenonsi, M., Dupont, S., Braghetta, P., Broccoli, V., Hassan, A. B., Volpin, D., Bressan, G. M. and Piccolo, S. (2003). Mapping Wnt/beta-catenin signaling during mouse development and in colorectal tumors. *Proc. Natl. Acad. Sci. USA* **100**, 3299-3304.
McKeown, S. J., Lee, V. M., Bronner-Fraser, M., Newgreen, D. F. and Farlie, P. G. (2005). Sox10 overexpression induces neural crest-like cells from all dorsoventral levels of the neural tube but inhibits differentiation. *Dev. Dyn.* **233**, 430-444.
McMahon, A. P. and Bradley, A. (1990). The Wnt-1 (int-1) proto-oncogene is required for development of a large region of the mouse brain. *Cell* **62**, 1073-1085.
Merrill, B. J., Pasolli, H. A., Polak, L., Rendl, M., Garcia-Garcia, M. J., Anderson, K. V. and Fuchs, E. (2004). Tcf3: a transcriptional regulator of axis induction in the early embryo. *Development* **131**, 263-274.
Meyers, E. N., Lewandoski, M. and Martin, G. R. (1998). An Fgf8 mutant allelic series generated by Cre- and Flp-mediated recombination. *Nat. Genet.* **18**, 136-141.
Mukhopadhyay, M., Shtrom, S., Rodriguez-Esteban, C., Chen, L., Tsukui, T., Gomer, L., Dorward, D. W., Glinka, A., Grinberg, A., Huang, S. P. et al. (2001). Dickkopf1 is required for embryonic head induction and limb morphogenesis in the mouse. *Dev. Cell* **1**, 423-434.
Ombrato, L., Lluis, F. and Cosma, M. P. (2012). Regulation of self-renewal and reprogramming by TCF factors. *Cell Cycle* **11**, 39-47.
Park, D.-S., Seo, J.-H., Hong, M., Bang, W., Han, J.-K. and Choi, S.-C. (2013). Role of Sp5 as an essential early regulator of neural crest specification in Xenopus. *Dev. Dyn.* **242**, 1382-1394.
Rodríguez, C. I., Buchholz, F., Galloway, J., Sequerra, R., Kasper, J., Ayala, R., Stewart, A. F. and Dymecki, S. M. (2000). High-efficiency deleter mice show that FLPe is an alternative to Cre-loxP. *Nat. Genet.* **25**, 139-140.
Saint-Jeannet, J.-P., He, X., Varmus, H. E. and Dawid, I. B. (1997). Regulation of dorsal fate in the neuraxis by Wnt-1 and Wnt-3a. *Proc. Natl. Acad. Sci. USA* **94**, 13713-13718.
Sakai, D., Tanaka, Y., Endo, Y., Osumi, N., Okamoto, H. and Wakamatsu, Y. (2005). Regulation of Slug transcription in embryonic ectoderm by beta-catenin-Lef/Tcf and BMP-Smad signaling. *Dev. Growth Differ.* **47**, 471-482.
Sakai, D., Suzuki, T., Osumi, N. and Wakamatsu, Y. (2006). Cooperative action of Sox9, Snail2 and PKA signaling in early neural crest development. *Development* **133**, 1323-1333.
Sandell, L. L., Butler Tjaden, N. E., Barlow, A. J. and Trainor, P. A. (2014). Cochleovestibular nerve development is integrated with migratory neural crest cells. *Dev. Biol.* **385**, 200-210.
Satoh, K., Kasai, M., Ishidao, T., Tago, K., Ohwada, S., Hasegawa, Y., Senda, T., Takada, S., Nada, S., Nakamura, T. et al. (2004). Anteriorization of neural fate by inhibitor of beta-catenin and T cell factor (ICAT), a negative regulator of Wnt signaling. *Proc. Natl. Acad. Sci. USA* **101**, 8017-8021.
Shy, B. R., Wu, C.-I., Khramtsova, G. F., Zhang, J. Y., Olopade, O. I., Goss, K. H. and Merrill, B. J. (2013). Regulation of Tcf7l1 DNA binding and protein stability as principal mechanisms of Wnt/beta-catenin signaling. *Cell Rep.* **4**, 1-9.
Simoes-Costa, M. and Bronner, M. E. (2015). Establishing neural crest identity: a gene regulatory recipe. *Development* **142**, 242-257.
Simões-Costa, M., Stone, M. and Bronner, M. E. (2015). Axud1 integrates Wnt signaling and transcriptional inputs to drive neural crest formation. *Dev. Cell* **34**, 544-554.
Steventon, B. and Mayor, R. (2012). Early neural crest induction requires an initial inhibition of Wnt signals. *Dev. Biol.* **365**, 196-207.
Steventon, B., Araya, C., Linker, C., Kuriyama, S. and Mayor, R. (2009). Differential requirements of BMP and Wnt signalling during gastrulation and neurulation define two steps in neural crest induction. *Development* **136**, 771-779.
Taneyhill, L. A. and Bronner-Fraser, M. (2005). Dynamic alterations in gene expression after Wnt-mediated induction of avian neural crest. *Mol. Biol. Cell* **16**, 5283-5293.
Thomas, K. R. and Capecchi, M. R. (1990). Targeted disruption of the murine int-1 proto-oncogene resulting in severe abnormalities in midbrain and cerebellar development. *Nature* **346**, 847-850.
Travis, A., Amsterdam, A., Belanger, C. and Grosschedl, R. (1991). LEF-1, a gene encoding a lymphoid-specific protein with an HMG domain, regulates T-cell receptor alpha enhancer function [corrected]. *Genes Dev.* **5**, 880-894.
Vallin, J., Thuret, R., Giacomello, E., Faraldo, M. M., Thiery, J. P. and Broders, F. (2001). Cloning and characterization of three Xenopus slug promoters reveal direct regulation by Lef/beta-catenin signaling. *J. Biol. Chem.* **276**, 30350-30358.
van de Wetering, M., Oosterwegel, M., Dooijes, D. and Clevers, H. (1991). Identification and cloning of TCF-1, a T lymphocyte-specific transcription factor containing a sequence-specific HMG box. *EMBO J.* **10**, 123-132.
Wu, J., Yang, J. and Klein, P. S. (2005). Neural crest induction by the canonical Wnt pathway can be dissociated from anterior–posterior neural patterning in Xenopus. *Dev. Biol.* **279**, 220-232.
Wu, C.-I., Hoffman, J. A., Shy, B. R., Ford, E. M., Fuchs, E., Nguyen, H. and Merrill, B. J. (2012). Function of Wnt/beta-catenin in counteracting Tcf3 repression through the Tcf3-beta-catenin interaction. *Development* **139**, 2118-2129.
Zhao, T., Gan, Q., Stokes, A., Lassiter, R. N. T., Wang, Y., Chan, J., Han, J. X., Pleasure, D. E., Epstein, J. A. and Zhou, C. J. (2014). beta-catenin regulates Pax3 and Cdx2 for caudal neural tube closure and elongation. *Development* **141**, 148-157.

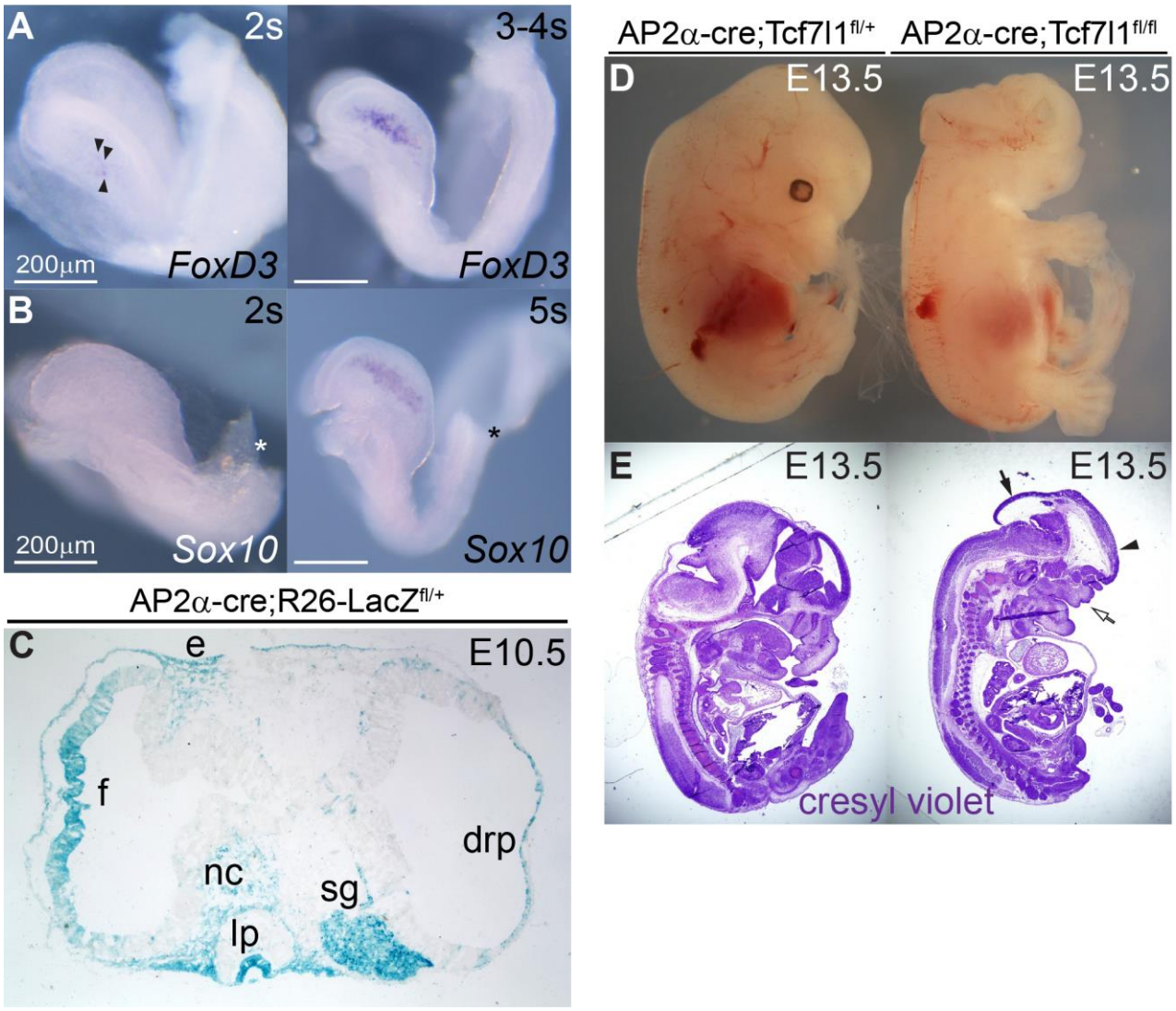

Fig. S1. Expression of NC genes at E8 and gross morphology of AP2α-Cre;Tcf7l1$^{fl/fl}$ mutants embryos. (A,B) Expression of NC genes during early mouse embryogenesis. RNA *in situ* hybridisation of *FoxD3* at stages 2s and 3-4s (A) and *Sox10* at stages 2s and 5s (B). * artefact caused by embryo dissection. **(C)** Mapping of AP2α-Cre recombination activity. A transverse section of AP2α-Cre;Rosa26$^{LacZfl/+}$ embryo at E10.5. Cre activity was detected using β-galactosidase enzyme assay. **(D)** Tcf7l1 deletion results in exencephaly. **(E)** Histological analysis of sagittal sections from the AP2α-Cre;Tcf7l1$^{fl/fl}$ "strong" mutant at E13.5 sections stained with cresyl violet show severe defects in the splanchnocranium, the forebrain (arrowhead) and midbrain (arrow).

Drp, dorsal roof plate; e, surface ectoderm; f, forebrain; lp, lens pit; nc-neural crest; sg, sensory ganglion.

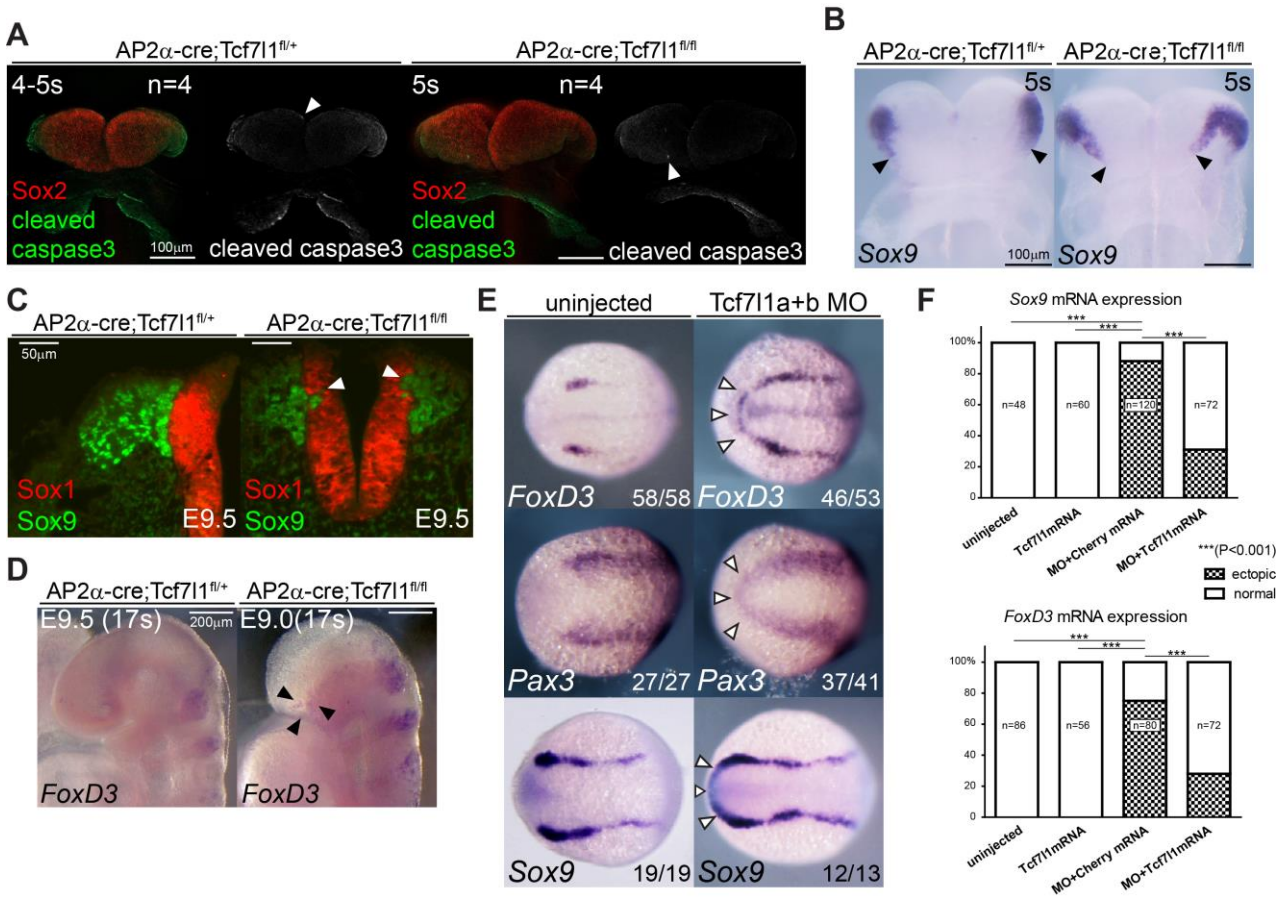

Fig. S2. Expansion of NC markers after ablation of Tcf7l1 in mouse and zebrafish. **(A)** Apoptosis is not altered in Tcf7l1 mouse mutant embryos at 5s stage as analyzed by immunofluorescence using anti-Caspase3 antibody, frontal view on the ANF, arrowheads points at one positive cell in each embryo. **(B)** *Sox9* mRNA expands rostrally in AP2α-Cre;Tcf7l1$^{fl/fl}$ mutant at 5s stage. Expansion of *Sox9* is marked by arrowheads. **(C)** Immunohistological staining of transverse sections from the hindbrain at E9.0 revealed ectopic Sox9-positive/Sox1-negative cells (arrowheads) in AP2α-Cre;Tcf7l1$^{fl/fl}$ mutants. **(D)** Aberrant *FoxD3* mRNA expression (arrowheads) in Tcf7l1 conditional mutants at E9.0. **(E)** Morpholino (MO) knock-down of Tcf7l1a and Tcf7l1b variants in zebrafish at 12hpf stage. Expression of *FoxD3*, *Pax3* and *Sox9* mRNA expands anteriorly along the anterior NPB in Tcf7l1 morphants (arrowheads). **(F)** Rescue of Tcf7l1 morphants using co-injection of mouse Tcf7l1 mRNA and control mRNA Cherry. Quantification of the ectopic expression shown in (E, arrowheads) and normal pattern of Sox9 and FoxD3 transcripts. Statistical significance was calculated using Fishers test.

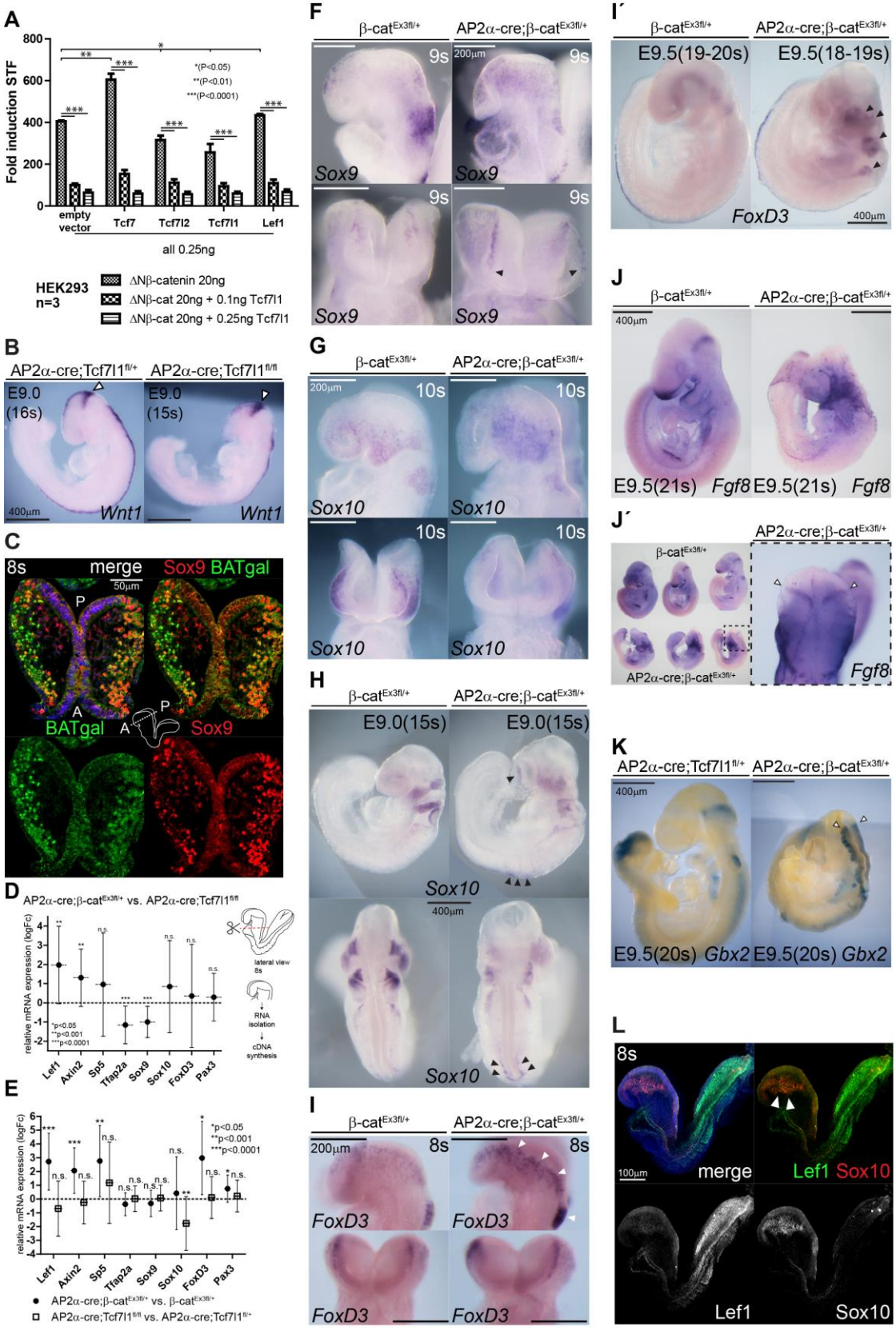

Fig. S3. Analysis of NC cells in AP2α-Cre;β-cat$^{Ex3fl/+}$ embryos. (A) SuperTopFlash luciferase reporter assay in HEK293 cells documents Tcf7l1 ability to repress Tcf/Lef driven gene expression. Activation of the pathway was achieved by co-transfection with non-degradable form of β-catenin (ΔNβ-catenin). Statistical significance was calculated using Student´s *t*-test. Error bars indicate ± SD. **(B)** The expression of *Wnt1* transcripts is unchanged in the MHB (arrowhead) of AP2α-Cre;Tcf7l1$^{fl/fl}$ mutants at E9.0. **(C)** Sox9 and BAT-gal immunostaining of transverse sections of 8s wild-type embryos. Please note the large overlap between the Sox9-positive and BAT-gal-positive delaminating cells. Nuclei were counterstained with DAPI. **(D)** qRT-PCR graph showing differential expression of Wnt target genes and genes involved in the NC induction and specification. Samples from dissected heads of the AP2α-Cre;β-cat$^{Ex3fl/+}$ vs. AP2α-Cre;Tcf7l1$^{fl/fl}$ mutants at 6-12s stage, n=6 for each genotype. Values are in log2 scale, Statistical significance was calculated by a two-tailed Student's *t*-test. Error bars indicate ± SD. **(E)** qRT-PCR graph showing differential expression of Wnt target genes and genes involved in the NC induction and specification. Samples from dissected heads of the AP2α-Cre;β-cat$^{Ex3fl/+}$ vs. β-cat$^{Ex3fl/+}$ (full circles) and AP2α-Cre;Tcf7l1$^{fl/fl}$ vs. AP2α-Cre;Tcf7l1$^{fl/+}$ (empty squares) at 6-12s stage, n=5 for each genotype. Values are in log2 scale, Statistical significance was calculated by a two-tailed Student's *t*-test. Error bars indicate ± SD. **(F-G)** RNA *in situ* hybridisation of *Sox9* (F) and *Sox10* (G) in AP2α-Cre;β-cat$^{Ex3fl/+}$ mutants showing anterior expansion of *Sox9* (arrowheads) but reduced and more dispersed expression of *Sox10* at 8s stage. Side (top) and frontal view (bottom). **(H)** *Sox10* is expressed in higher levels in the anterior head and caudal trunk (arrowheads) of the AP2α-Cre;β-cat$^{Ex3fl/+}$ mutants than in the controls at E9.5. Side (top) and frontal view (bottom). **(I,I´)** *Foxd3* expression is more abundant in AP2α-Cre;β-cat$^{Ex3fl/+}$ mutants than in the controls at 8s (white arrowheads) (I) and E9.5 stage (black arrowheads). Side (top) and frontal view (middle) are shown at 8s stage, and side (bottom) view is shown for E9.5 (I´). **(J-J')** *Fgf8* mRNA is abnormally spread in large areas around branchial arches but it is detected in the MHB (arrowheads) of AP2α-Cre;β-cat$^{Ex3fl/+}$ mutants. **(K)** MHB marker *Gbx2* is ectopically expressed caudally from MHB (marked by arrowheads) in the AP2α-Cre;β-cat$^{Ex3fl/+}$ mutants at E9.5. **(L)** Whole mount immunofluorescence showing overlapping expression of Lef1 and Sox10 in NC cells (arrowheads) in wild-type embryo at 8s stage. Nuclei were stained with Hoechst.
A, anterior; P, posterior.

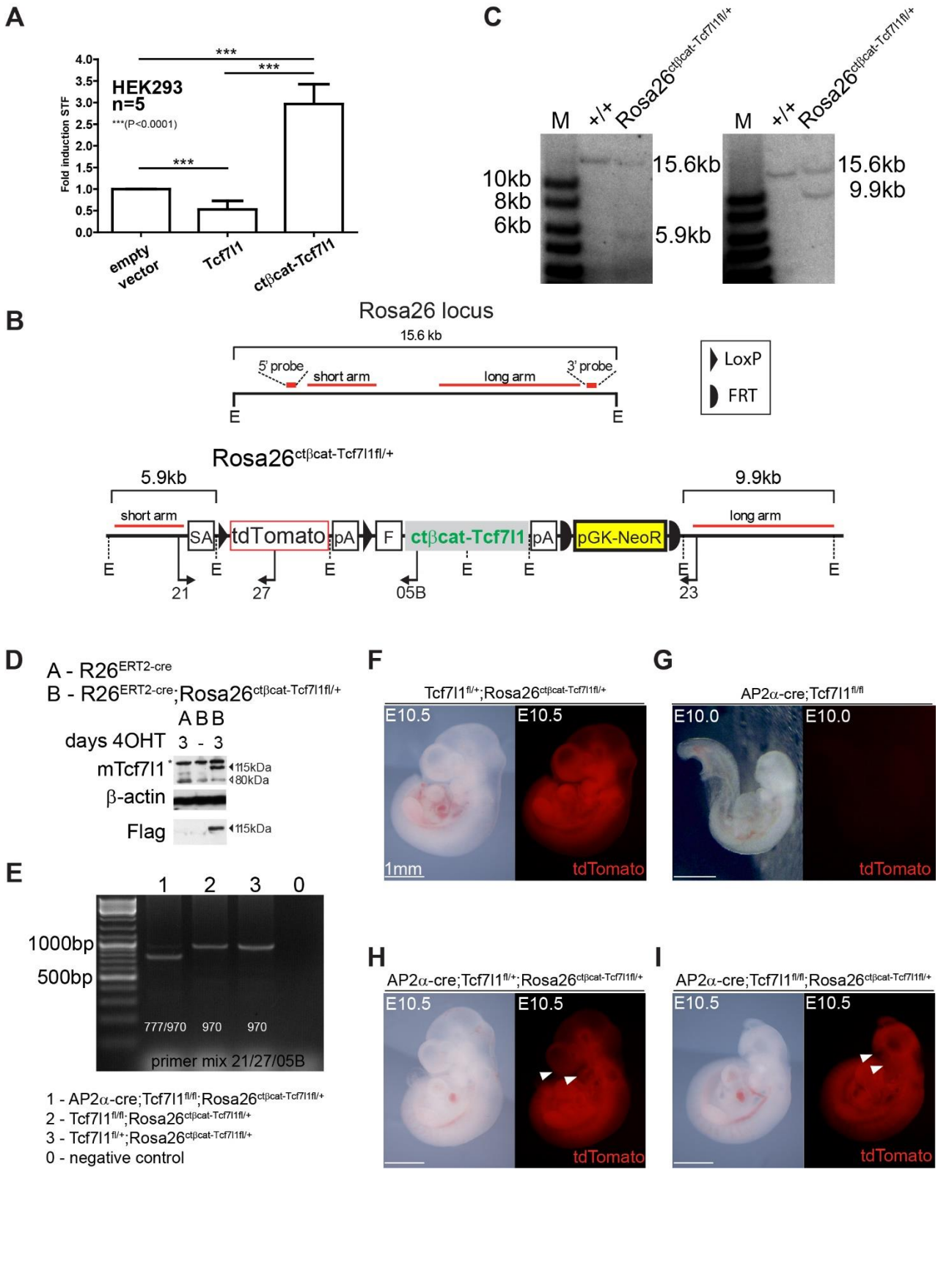

Fig. S4. Generation and validation of the mouse strain Rosa26$^{ctβcat\text{-}Tcf7l1fl/+}$. (A) SuperTopFlash assay in HEK293 cells shows ctβcat-Tcf7l1 mediated activation and Tcf7l1 mediated repression of the Tcf/Lef reporter. Statistical significance was calculated using Student´s *t*-test. Error bars indicate ± SD. **(B)** Scheme of the Rosa26 locus and the targeting vector, homology arms are depicted in red. **(C)** Southern blotting analysis confirms correct homologous recombination in ES cells, short arm is on the left. **(D)** Western blotting of lysates from mouse embryonic fibroblasts (MEFs) isolated from the R26$^{ERT2\text{-}cre}$;Rosa26$^{ctbcat\text{-}Tcf7l1fl/+}$ embryos revealed the presence of the ctβcat-Tcf7l1 fusion protein 3 days after administration of 4-OHT (4-*hydroxitamoxifen*). Size of the endogenous Tcf7l1 is approximately 80kDa, ctβcat-Tcf7l1 protein size is around 115kDa. **(E)** PCR confirmation of Cre recombination in AP2α-Cre;Tcf7l1$^{fl/fl}$; Rosa26$^{ctβcat\text{-}Tcf7l1fl/+}$ compound mutants, resulting size of the PCR products was 970bp prior and 777bp after recombination**. (F-I)** Rosa26$^{ctbcat\text{-}Tcf7l1fl/+}$ mice ubiquitously express fluorescent protein tdTomato. The loss of its expression upon Cre recombination is marked by arrowheads in the AP2α-Cre;Tcf7l1$^{fl/fl}$;Rosa26$^{ctβcat\text{-}Tcf7l1fl/+}$ embryos (H) and the AP2α-Cre;Tcf7l1$^{fl/fl}$;Rosa26$^{ctβcat\text{-}Tcf7l1fl/+}$ compound mutants (I). AP2α-Cre;Tcf7l1$^{fl/fl}$ serves as a negative control (G).

E, EcoRI cleavage site; SA, splice acceptor; pA, poly-adenylation signal; pGK-NeoR, neomycin expressing cassette; F, Flag tag sequence;*, non-specific binding of the antibody; primers for genotyping 21-JM21F, 23-JM23R, 27-JM27R, 05-JM05B.

Supplemental Table S1 (Related to Materials and methods)

ISH probes		
Gene	forward	reverse
FoxD3	GGACCGCAAGAGTTCGCGGA	TCCGGAGCTCCCGTGTCGTT
Sox9	GAGCACTCTGGGCAATCTCAG	CTCAGGGTCTGGTGAGCTGTG
Gbx2	Gift from Peter Rathjen	Adelaide University
Sp5	CGTGAAGACGCACCAAAATA	TATTTTCACGCTGCCAACTG
Fgf8	CAGGTCCTGGCCAACAAG	GAGCTCCCGCTGGATTCCT
Sox10	Gift from Anthony Firulli	Indiana University, USA
Sox2	Open Biosystems	BC057574
FoxG1	Gift from Stefan Krauss	OUS, Oslo, Norway
Six3	Gift from Guillermo Oliver	St. Jude Hospital, Memphis, USA
Wnt1	Gift from Andy McMahon	USC, USA
Tcf7l1	Open Biosystems	BC128306
Tcf7l2	Open Biosystems	BC052022
Pax3	ACTGTCTGTGATCGGAACACT	CTAGAACGTCCAAGGCTTACT

Antibodies		
Gene	Company	Dilution
Sox1	RαD AF3369	1:1000
Tfap2α	Sanαta Cruz Biotech SC-184	1:1000
Sox10	Santa Cruz Biotech SC-17342	1:1000
Sox9	Millipore AB5535	1:2000
N-cadherin	BD Transduction Lab. 610920	1:2000
GFP	Life Technologies A11122	1:1000
β-galactosidase	Abcam ab9361-250	1:1000
Lef1	Cell Siganling C12A5	1:1000
cleaved caspase-3	Cell Signaling 9664	1:2000
qPCR Primers		
Axin2	AGCTTCCGCGAGGATGCTCC	TGCACCAATCCTGGTCACCCA
Tfap2	CACGAGGACCTCTTGCACGG	GTTGGACTTGGACAGGGACA
Sox9	AGGAAGCTGGCAGACCAGT	TCCACGAAGGGTCTCTTCTC
Sox10	ATGTCAGATGGGAACCCAGA	CACGTTGCCGAAGTCGATGT
Pax3	AGGAGGCGGATCTAGAAAG	TCAGCGGTAAATCAGGTTCA
Sp5	AAGCAACACGTGTGCCACGT	GTCTTCACGTGCTTGGCGAG
FoxD3	ATCCTGGTCCATCTGTCCTG	GTAATCCGGGTGTTCCTTCA
Lef1	CCTTTCTCCACCCATCCCGA	ACAGGCTGACCTTGCCAGCC